

UNCLASSIFIED

AD NUMBER
AD838966
NEW LIMITATION CHANGE
TO Approved for public release, distribution unlimited
FROM Distribution authorized to U.S. Gov't. agencies and their contractors; Critical Technology; APR 1968. Other requests shall be referred to Office of Naval Research, 875 North Randolph Street, Arlington, VA 22203.
AUTHORITY
NSRDC ltr dtd 12 Oct 1972

THIS PAGE IS UNCLASSIFIED

9968396  
AD 8388  
AD 8388

①

DETERMINATION OF THE SPECIFIC DAMPING  
ENERGY OF SHIP HULL JOINTS,  
AND ITS EFFECT ON NOISE RADIATION

-----  
Navy Contract Nonr - 401(49)

-----  
Final Report

-----  
April, 1968

-----  
W. McGuire

-----  
Department of Structural Engineering  
School of Civil Engineering  
Cornell University  
Ithaca,  
New York

This document is subject to special  
export controls and each transmittal  
to foreign governments or foreign  
persons may be made only with a letter  
of authorization from the Director,  
Naval Hydromechanics  
Naval Ship Research  
Washington, D.C. 20340

INTRODUCTION. Noise transmitted into the water through the hull of a ship is generated mainly by the machinery within the ship. The noise energy is conducted into the hull either by conduction through the structure or through the air. Damping of the energy and reduction in the amount transmitted to the water is desirable. One possible means of damping is through energy absorption in the material (frames and plates). Tests have shown that material damping is insignificant when the vibratory strains are as low as they would be in normal ship operation. A second possibility is damping through the attachment of coatings and blankets to the hull. This has been and is being investigated extensively by others. A third possibility is damping in the structural joints. The aim of the investigation reported herein is to make some contribution toward the further understanding of joint damping.

The project and this report can be conveniently divided into three parts:

- I. Comparative study of different joint configurations.
- II. Experimental study of bolted butt splices.
- III. Analytical study of bolted butt splices.

PART I

COMPARATIVE STUDY OF DIFFERENT JOINT CONFIGURATIONS

This phase of the investigation was carried out under the direction of Doctor Robert O. Fehr. It was an experimental study of the dissipation of vibratory energy in joints of various designs. An attempt was made to determine those parameters which influence joint damping significantly. The following account of these tests is taken from Professor Fehr's earlier report (Reference 1).

Instrumentation: Tests were conducted on beams, and on cylinders, with and without joints. For the tests, the beams and cylinders were suspended in such a way that the energy dissipated by the mounting and by the measuring equipment was kept at a minimum. The beams were vibrated in the "free-free" beam mode. The beams were supported on knife edges located in the nodal planes, and excited by an electromagnet to vibrate at their natural frequency. The vibration displacement of the beam decayed when the power to the magnets was cut. The decay of the amplitude of displacement was traced by a strip chart recorder. A capacity type vibration detector was used as a sensor (See Fig. 1).

The quality factor  $Q$  obtained for an integer beam was measured as 6200, corresponding to a logarithmic

decrement of  $\delta = \pi/Q.0005$ . This value has the order of magnitude reported for material damping in the literature. Hence, this type of instrumentation was considered to be satisfactory for the present purpose. It should be mentioned that attaching a small accelerometer to the beam for sensing displacement increased the damping to a  $Q = 1500$ . Attempts were also made to measure the damping by means of a mechanical impedance head. The mechanical impedance measured was then converted into values of  $Q$ . For this conversion it is necessary to know the mechanical energy stored in the beam. This energy was calculated from displacement and frequency readings measured with a microscope and a frequency counter respectively. Satisfactory agreement between the measurements taken with the mechanical impedance head and by the decrement method was obtained for values of damping where  $Q$  had a value below 300. The stresses in the structures were held low; in this range only insignificant changes of damping with vibration amplitude were observed.

Tests. Tests were conducted on integer beams as reference, welded beams, and bolted beams. The tests were conducted on beams  $3\frac{1}{2}$ " and 4" wide x  $\frac{3}{8}$ " thick x 25.5" long at a frequency of approximately 100 cps. The materials was SAE 1020 (.18/.23 C; .4/.6 Mn; .04  $P_{max}$ ; .05  $S_{max}$ ; hot rolled). The peak-to-peak vibration displacements of the integer as well as of the welded beams were held

to a value corresponding to a stress amplitude of about 2500 psi. Figure 2 shows the type of beams tested and the quality factor Q obtained. (Other results are shown on Figures 3 to 9.) Each value of Q given in Figure 2 is the average of a large number of measurements. As expected, the damping of the bolted joints changed with clamping pressure. Hence, tests were conducted at various bolt torques and amplitudes of displacement. A change of surface finish also caused a change of the damping.

In order to test the effect of configuration, a test series was started for determining the damping of welded cylinders. Figure 2 indicates also results obtained from damping tests on such a configuration.

Discussion. The dissipation of vibrating energy in a butt welded joint is very small when the weld metal is steel. Judging from a very small sample, the energy dissipation may vary over a range of 1 to 3 for individual welds of the same type. The reason for this variation was not explored.

Introduction of a welding material of high material damping increases the energy dissipation in the joint. We do not know of any weld material of high internal damping which may be used for making a strong weld. A lead alloy was used as weld metal just to demonstrate that welds of high dissipation of vibrational energy could be made, if a suitable material could be found.

Since damping depends on the ratio of the energy dissipated to the energy stored, it became inherently more difficult to obtain high damping for heavier sections. We have tried to estimate the length of weld (steel weld) which would be required to reduce the quality factor  $Q$  of cylinders to a value of 50. The energy dissipation of a weld was assumed to be proportional to its length. The order of magnitude figures for such a weld length were calculated as 400 ft. for a cylinder of  $D = 9.36"$ ,  $L = 7.5"$  and  $t = .28"$ , and as 1200 ft. for a cylinder of  $D = 15$ ,  $L = 10'$  and  $t = 4"$ . These results indicate that the use of welds for introducing damping of any significance is impractical.

Considerably higher damping constants were achieved by introducing bolted joints. The damping of bolted joints is higher by an order of magnitude than the damping of welded joints. In addition to vibration amplitude, variations of type of joint, clamping pressure, and surface finish have a considerable effect on damping. Surfaces of lower roughness value appear to dissipate more energy, apparently due to greater slippage between the surfaces. Mill scale on the surfaces permits more slippage, and hence higher energy dissipation in the joint (see Figure 9).

The contact area of the edges of the two beams may be changed to increase the damping of a bolted butt joint.

Interesting results were obtained with a "V"-shaped butt joint where a compressive force was used to push the edges of the beams together (Figure 6).

## PART II

### EXPERIMENTAL STUDY OF BOLTED BUTT SPLICES

Review of the above work of Professor Fehr led the writer and Dr. S. J. Errera, to conclude that a systematic investigation of the simple and rather basic steel model shown in Figure 10 would be the logical next step in the investigation started by Fehr. In such a study attention should be focused on the phenomenon of interfacial slip damping in steel plates. The model is a flat bar supported and excited as in Fehr's tests. Clamped to the two faces of the bar are plates of length  $l$ , thickness  $h$ , and the same width as the main bar. Uniform clamping pressure is approximated by pretensioned bolts running through all three plates. In addition to lending itself to testing, the model is amenable to approximate analysis. The effect of varying the dimensional parameters  $t$ ,  $h$ , and  $l$ , as well as the contact pressure, surface friction, stress amplitude and frequency can be studied. Investigation of spliced plates of similar configuration naturally follows the study of the simple model of Figure 10. An account of this phase of the project follows. Most of the experimental and analytical work

was done by Mr. H. Yang, Research Assistant, and the account is taken from an earlier report by Yang, Errera and McGuire (Reference 2).

Tests and Analysis. In addition to purely experimental work, a theoretical method for predicting natural frequencies and nodal point positions of test specimens was used for comparison with test results.

The eight specimen configurations tested are shown in Figure 11. Top and side views of specimens "a" and "f" are shown in Figure 12. Each specimen is a  $3\frac{1}{2}$  x  $\frac{3}{8}$ " cold rolled steel bar spliced with  $3\frac{1}{2}$ " x  $\frac{3}{16}$ " plates and  $\frac{1}{2}$ " diameter high strength bolts. The bolt holes are  $\frac{9}{16}$ " diameter so that enough gap is provided for slip motion to occur. The liner plates added in specimens "c", "g", and "h" are cold rolled steel plates with 0.05" thickness. The retaining bolts in specimens "f" and "h" are only lightly torqued (5 to 20 ft-lb) and their holes are  $\frac{1}{8}$ " oversize to insure the sliding motion between the splice plates and main plates is not hindered.

When the specimens were assembled, bolt elongation readings were taken and compared with calibration curves for bolts of the same size to check the bolt tension.

Theoretical Prediction of Natural Frequency and Position of Nodal Points. For a beam of constant cross section over its length, the deflected shape during free vibration

can be considered to be a sine wave. For the specimens tested, the cross section is not constant over the full length, and the deflected shape deviates from a sine wave. Stodola's Graphical Method (Reference 3) was used to predict the natural frequency of each specimen and its real deflected shape as well.

Sample deflection curves obtained by Stodola's Method are shown in Figure 13. Each corresponding sine curve is also shown. It is seen that the Stodola curves are flatter than the corresponding sinusoidal curves.

The natural frequencies obtained by Stodola's method are in very good agreement with those obtained by experiments; the differences are less than 10%.

The nodal positions of the specimens can be determined theoretically by setting total vertical momentum equal to zero. In calculating the vertical momentum, the deflected shape was assumed to be a sine wave, so that the calculation involved only simple calculus. The nodal position thus obtained, though not precise, gave approximate starting points for locating the real positions experimentally.

Damping Dependence on Amplitude. In the tests made, it has been observed that the energy lost per cycle of vibration obeys the following law reasonably well:

$$\Delta W = K\delta^n \quad (1)$$

where

$\Delta W$  = energy loss per cycle

$\delta$  = amplitude of deflection

$K, n$  = factors for each specimen

The exponent  $n$  has been found to lie between the limits of 2.3 and 2.8 in the specimens tested. Figure 14 is a re-plot on a log-log scale of Figure 4. Figure 14 shows the power law dependence more clearly than did the original semi-log plot. Figure 15 is typical of the results obtained in this series of tests. The specimen is a  $3\frac{1}{2}$ " x  $3/8$ " cold rolled steel bar spliced with  $3\frac{1}{2}$ " x  $3/16$ " plates and  $\frac{1}{2}$ " high strength bolts. In Figure 15, the ordinates are values which are proportional to  $\Delta W$ , i.e.  $1000\delta^2/Q$ , rather than  $\Delta W$ . This choice of coordinates is used to emphasize the measured quantities used in plotting the curves and also because of some questions as to the accuracy of the methods available for calculating the absolute values of  $\Delta W$ . Figure 16 contains additional results.

Numerous studies of material damping in steel have demonstrated that Eq. (1) is a satisfactory representation of material damping at low to intermediate stress levels (Reference 4). Data on interfacial slip damping, the predominant mechanism in this series of tests, are not so plentiful however. One of the latest reviews of the subject (Reference 5) indicates that theoretically, at

least for some types of joints, the energy dissipated in slip damping is proportional to the cube of the stress range.

The total energy dissipated in the beam per cycle can be expressed as:

$$\Delta W = \frac{2\pi W}{Q} \quad (2)$$

where  $W$  = stored energy  
and  $Q$  = quality factor

The stored energy,  $W$ , can be obtained by

$$W = 1/2 \int mv^2 = \frac{\omega_n^2}{2} \int_0^l \mu y^2 dx \quad (3)$$

where  $\mu$  = mass per unit length  
and  $y$  = the deflection along the length of the beam

It is suggested here that the ordinates measured from Stodola's deflection curves be used to evaluate the stored energy. It was pointed out earlier that this  $y$  value appears to have very good accuracy. Simpson's Rule can be used in the process of numerical integration of Eq. 3.

The quality factor,  $Q$ , of a  $3\frac{1}{2}$ " x  $3/8$ " x 26" cold rolled integer steel beam has been measured as 6200. Once the value of total energy loss per cycle,  $\Delta W$ , has been found from Eq. (2), the energy loss in the joint per cycle,  $\Delta W_{\text{joint}}$ , is

$$\Delta W_{\text{joint}} = 2\pi W \left( \frac{1}{Q} - \frac{1}{Q_{\text{reference}}} \right) \quad (4)$$

where

$$Q_{\text{reference}} = 6200.$$

Calculations using this approach have indicated that the energy loss per cycle for a jointed beam (specimen "f") is 20 to 50 times as large as the loss for a solid beam of the same dimensions.

Effect of Bolt Tightness. Tests were conducted on each of the eight specimens with bolt torques varying from 10 to 90 ft-lb. The results indicated that the bolt tightness had no effect on the natural frequency and nodal positions.

The damping energy per cycle (in terms of  $1000\delta^2/Q$ ) was determined for each specimen at various values of bolt torque and deflection amplitude. In Table 1 the results are compared at a deflection of  $\delta = .004$ ", and it is seen that when bolt tightness increases from 10 ft-lb to 50 ft-lb, the damping energy decreases about 36 to 62%.

Table 1 Energy dissipated per cycle ( $1000\delta^2/Q$ ) when  
 $\delta = .004"$

Bolt Torque Specimen	10 ft-lb	50 ft-lb		90 ft-lb	
	(D.E.)	(D.E.)	P	(D.E.)	P
a	40	25.5	36.2%	20	50 %
b	100	41	59 %	28.5	71.5%
c	100	34.5	65.5%	28	72 %
d	63	27.5	56.4%	14.5	77 %
e	55	32	61.5%	25.5	69.3%
f	112	54	51.8%	33.5	70 %
g	62	31	49.7%	26	58 %
h	78	39	50 %	25.5	67.3%

where D.E. = Damping energy per cycle in terms of  $1000\delta^2/Q$   
when  $\delta = .004"$

and P = Decreasing percentage of D. E. when compared  
with D.E. in the case of 10 ft-lb bolt torque.

Similarly, when bolt torque increases from 10 ft-lb to 90 ft-lb, the damping energy decreases about 50 to 77%. Typical graphs of Q versus bolt tightness are shown in Figure 17 for specimen "f".

Effect of Splice Plate Length. Theory indicates that the natural frequency of a specimen increases as the splice plate increases in length, and that the nodal points move toward the ends. The test results are in agreement with the theoretical predictions.

The damping energy per cycle (in terms of  $1000\delta^2/Q$ ) is listed in Table 2 for specimens "b", "e" and "f" at prescribed values of bolt torque and amplitude. Comparison

of specimens "b" and "e" indicate that the damping energy is less for the longer splice plates, specimen "e". This difference decreases with increasing bolt torque. This is because, for low bolt torque, in the

Table 2. Comparison of Damping Energy of Specimen b, e, and f.

Bolt Torque (ft-lb)	Specimen Amplitude $\delta$	b		e		f	
		(1) Energy Dissi.	(1) Energy Dissi.	(2) Compared with (b)	(1) Energy Dissi.	(2) Compared with (b)	
10 ft-lb	.0015 in	7.8	5.5	-29 %	9.4	+20.5%	
	.0035 in	72	41	-43 %	80	+11.1%	
	.006 in	260	145	-44 %	340	+31 %	
50 ft-lb	.0015 in	4.0	3.1	-22.5%	4.0	+ 0 %	
	.0035 in	32	25	-22 %	37	+15.6%	
	.006 in	116	78	-33 %	152	+31 %	
90 ft-lb	.0015 in	5.3	4.5	-17 %	5.3	+ 0 %	
	.0035 in	28	26	- 7.1%	34	+21.4%	
	.006 in	150	150	- 0 %	226	+51 %	

Note: Energy dissipation per cycle is in term of  $1000\delta^2/Q$ .

central region of specimen "e" interfacial contacting area and contacting pressure were lacking between the splice plates and main plates. In fact, it was possible to slide a piece of paper into the gap between the splice and main plates in the central region of the specimen. Thus the extremely low friction of the slip motion causes relatively low damping.

Effect of Retaining Bolts. Specimens "e" and "f" are identical except that specimen "f" had two extra

retaining bolts in the central section. These retaining bolts were lightly torqued (5 to 20 ft-lb), and their holes provided 1/8" clearance so that sliding between the splice plates and the main plates was not hindered. When the long spliced specimen was clamped loosely with retaining bolts, both the interfacial contacting area and the contacting pressure between the splice plates and the main plates was increased in the central region of the specimen. Thus it is seen from Table 2 that specimen "f" has much greater energy dissipation than specimen "e" (which had no retaining bolts), and also usually displayed greater energy dissipation than specimen "b" (which had shorter splice plates).

Earlier investigators have shown both theoretically and experimentally that there is an optimum value of retaining bolt tightness (References 6, 7). The present experiments have shown that this value is around 5 or 10 ft-lb for these specimens, which is an extremely low value for structural applications.

Effect of Liner Plates. Table 3 contains data on damping energy of specimens "e", "f", "g" and "h". Specimens "g" and "h" are made merely by adding 0.05" thick cold rolled steel liner plates to specimens "e" and "f", respectively.

Table 3. Effect of Liner Plates, Damping Energy per Cycle ( $1000\delta^2/Q$ ) when  $\delta = .004$

Bolt Torque \ Specimen	e	g	f	h
10 <sup>ft</sup> -lb	55	62	112	78
50	32	31	54	39
90	25.5	26	33.5	25.5

Comparison of "e" and "g" (specimens with no retaining bolts) indicates that the addition of liner plates has no effect on the damping energy. But comparison of "f" and "h" (specimens with retaining bolts) indicates that the addition of liner plates decreases the damping by about 25%. This effect may be caused by a difference in surface finish, or other factors causing a difference in the shear force necessary to produce slip.

The experimentally determined natural frequency and nodal positions were not affected materially by the addition of the very thin liner plates.

Effect of Surface Roughness. The specimens used consist of a  $3\frac{1}{2}$ " x  $\frac{3}{8}$ " x 30" cold rolled steel plate spliced with  $3\frac{1}{2}$ " x  $\frac{3}{16}$ " x 6" plates and eight  $\frac{1}{2}$ " high strength bolts. When investigating the effect of surface roughness, the interfaces of both the main and the splice plates of the joint are ground with grooves along the transverse direction of the specimen.

The tests made for determining the effect of surface roughness on damping show a definite trend. Figure 18 shows the influence of surface finish on quality factor Q. As seen from the Figure, with a certain surface roughness, such as 16, 23, 125, or 300 micro-inches, there is a consistent decrease in damping with increasing clamping pressure. It is also seen that, for a given clamping pressure, there is first an increase in damping with increasing surface roughness, and then a decrease. For clarity, a certain value of end deflection, such as 0.006 inches, is chosen so that we have a plot of the energy loss per cycle vs. interface roughness. As indicated in Figure 19a, there is an optimum value of surface finish (possibly around 63 micro-inches ground) for which the damping energy is maximum. A qualitative representation of Figure 19a is shown in Figure 19b. This is reasonable since for an ideally perfectly smooth surface (zero friction) the damping energy must be near zero and, on the other hand, for a very rough surface (high friction) the occurrence of slip motion is so difficult that the slip damping energy approaches zero.

Pian and Hallowell (Reference 6) have derived an expression of the energy loss per cycle of static load applied at the end of a cantilever beam which is similar to our case.

$$\Delta W/\text{cycle} = \frac{F^3 a^3}{12EIq_M h \left(1 + \frac{2I}{Ah^2} + \frac{F}{2q_M h}\right)^2} \quad (5)$$

where  $a$ ,  $E$ ,  $I$ ,  $h$ , and  $A$  are constant terms,  $F$  is vibration force, and  $q_M$  is the interfacial limiting shear force (proportional to the surface roughness for a given clamping pressure).

As can be seen from the formula, the energy loss per cycle is approximately proportional to  $q_M$  when the  $q_M$  value is relatively low, and energy loss per cycle is approximately in inverse proportion to  $q_M$  when the  $q_M$  value is relatively high. This formula, therefore, gives a convincing explanation of the results shown in Figure 19.

Effect of Rubber Layers. To investigate the effect of energy dissipating material, two pieces of rubber were clamped between the main and the splice plates of the same type of specimen as described in the preceding subsection. The tests conducted with the insertion of two pieces of rubber pad show the damping energy is increased enormously due to the absorption of energy by rubber.

A comparison of the damping energy of such a specimen with a specimen which has no rubber but with a surface roughness of 63 micro-inches is shown in Table 4 (again, the end deflection is 0.006 inches):

Table 4. Damping Energy ( $10^{-4}$  in-lbs.)

Bolt Types Tightness	(1) with pad rubber	(2) no pad rubber, 63 $\mu$ -in. ground	percentage increased by adding the pad rubber
10 ft-lbs	19.1	11.7	63%
50 ft-lbs	11.4	4.2	171%
90 ft-lbs	10.8	3.2	238%

Besides 1/16 inch thick rubber sheets, 1/8 inch thick ones were also used in the investigation. There was little difference in energy absorption.

### PART III

#### ANALYTICAL STUDIES OF BOLTED SPLICE

While affording useful data, the studies reported above led inevitably to the conclusion that further progress toward the understanding of joint damping required further analytical undergirding. Accordingly, an analytical investigation of a simple joint model was undertaken by Mr. Yang. Two methods were used, one based on an elementary strength of materials approach, the other using finite element techniques. The purpose was to develop and verify the finite element approach on a simple problem with the idea being that, once validated for a simple model, the powerful finite element approach could then be applied with reasonable assurance of success to more complex situations for which the simple methods would be completely inadequate. Following is an account of this work.

"Strength of Materials" Approach. As shown in Figure 20 the model used is a bileaf cantilever beam clamped with uniform pressure  $p$  per unit area. To establish a formula for finding the energy dissipation per cycle due to the cyclic free-end loading  $F$ , the following assumptions were made:

- 1) Either part of the beam behaves elastically when the load  $F$  is acting.
- 11) The static Coulomb friction coefficient equals the dynamic Coulomb friction coefficient. Namely,  $\mu = \mu_{\text{static}} = \mu_{\text{dynamic}}$ . Tests have shown that the kinetic coefficient of friction stabilizes after a few thousand cycles (Reference 5).

When a load is applied at the free end of the bileaf cantilever beam, the two individual pieces of such a beam will behave as one if the interfacial friction between the two pieces has not exceeded the static friction limit  $\mu p$ . The load-deflection relation is linear and can be shown as a straight line, see Figure 21 (line from 0 to 1).

Once the interfacial shearing stress between the two mating pieces, increasing with the increasing free-end load, has reached the static friction limit  $\mu p$ , slip starts to occur. As mentioned previously, the static friction coefficient is considered to be the same as

The dynamic friction coefficient. The occurrence of slip results in extra deflection above that of the "integer" beam. Consequently, the linear load-deflection line changes its slope after the limiting load ( $F_{slip}$ ), which causes slippage, has been reached. The line is shown in Figure 21 (from 1 to 2).

So far the load-deflection behavior has been described for a quarter of a loading cycle, namely, from zero to  $F_{max}$ . The load-deflection behavior of the remaining three quarters of the cycle can be considered similar by a complete hysteresis loop generated, as shown in Figure 22.

With the known ordinates of point 1 and 2, the area A of the triangle 0-1-2 can be calculated and, from this, the area of the whole loop.

The area A of the triangle 0-1-2 is:

$$A = \begin{vmatrix} 0 & 0 & 1 \\ \delta_{slip} & F_{slip} & 1 \\ \delta_{max} & F_{max} & 1 \end{vmatrix} = \frac{1}{2} (\delta_{max} \cdot F_{slip} - \delta_{slip} \cdot F_{max}) \quad (6)$$

When the free end load  $F$  is below  $F_{slip}$ , the two leaves behave as a whole. The horizontal shearing stress in the mid-depth is constant along the length of the beam and is equal to  $\frac{3}{2} \frac{F}{2th}$ . When  $F$  reaches  $F_{slip}$ , the mid-depth shearing stress increases to the value of  $\mu p$ .

$$\therefore \mu p = \frac{3}{2} \frac{F_{\text{slip}}}{2th} \quad F_{\text{slip}} = \frac{4}{3} \mu p t h \quad (7)$$

$\delta_{\text{slip}}$  is defined as the free end deflection caused by the free end load  $F_{\text{slip}}$ :

$$\delta_{\text{slip}} = \frac{F_{\text{slip}} l^3}{3EI} = \frac{2}{3} \frac{\mu p l^3}{Eh^2} \quad (8)$$

The maximum deflection can be obtained by two approaches:

- a)  $\delta_{\text{max}}$  is the superposition of the integer beam deflection ( $\delta_1$ ) and the deflection caused by slip ( $\delta_2$ ). See Figure 23.

$$\delta_1 = \frac{Fl^3}{3EI} = \frac{1}{2} \frac{Fl^3}{Eth^3} \quad (9)$$

For a constant vertical shear force  $F$ , the corresponding shearing stress at mid-depth of the integer beam with depth  $2h$  is:

$$v_{\text{mid-depth}} = \frac{3}{4} \frac{F}{Eh} \quad (10)$$

Subtracting the interfacial friction stress  $\mu p$ , which remains constant since slip has occurred, from the corresponding shearing stress at mid-depth caused by the load  $F$ , will give the interfacial friction which produce the additional end deflection  $\delta_2$ . The effective load, contributed by slip, and its corresponding moment diagram is thus shown in Figure 24.

$$A_1 = \frac{1}{4} \left( \frac{3}{4} \cdot \frac{F}{Eh} - \mu p \right) thl^2$$

$$\delta_2 = \frac{3}{4} \frac{l^3}{Eth^3} F - \frac{2\mu pl^3}{Eh^2}$$

$$\therefore \delta_{\max} = \delta_1 + \delta_2 = \frac{2l^3}{Eth^3} F - \frac{2\mu pl^3}{Eh^2} \quad (11)$$

b) As an alternative approach,  $\delta_{\max}$  can also be found by analyzing the free body of either one of the mating parts. The lower part of the beam is now analyzed. The free body loading condition is shown in Figure 25.

$$\delta_{\max} = \frac{Fl^3/2}{3EI} - \frac{2\mu pl^3}{Eh^2} = \frac{2l^3}{Eth^3} F - \frac{2\mu pl^3}{Eh^2} \quad (11)$$

Now,  $\delta_{\text{slip}}$ ,  $F_{\text{slip}}$ , and  $\delta_{\max}$  have all been found. Substituting them into equation (6).

$$A = \frac{2}{3} \frac{\mu ptl^2}{E} \left( \frac{3}{2} \frac{Fl}{th^2} - \frac{2\mu pl}{h} \right) \quad (12)$$

The damping energy per cycle is the area of a complete hysteresis loop and is eight times the area A (see Figure 22). Therefore:

$$\text{Damping per cycle} = \frac{16}{3} \cdot \frac{\mu ptl^2}{E} \left( \frac{3}{2} \frac{Fl}{th^2} - \frac{2\mu pl}{h} \right) \quad (13)$$

Finite Element Investigation. The "finite element method" is a general method of analysis in which a continuous structure is replaced by a finite number of elements interconnected at their corner nodal points. Continuity between elements is maintained by assuming that within each element straight edges originally straight remain straight after deforming. This is the same as assuming that the strain  $\epsilon_x$ ,  $\epsilon_y$  and  $\gamma_{xy}$  are constant within each element. The edge stress  $\sigma_x$ ,  $\sigma_y$  and  $\tau_{xy}$  are therefore also constant. These edge stresses are imagined to be replaced by resultant forces which act at the corners of the elements. Hence, it is possible to determine the stiffness of each element and obtain linear simultaneous equations which express the corner point loads in terms of corner point displacements.

$$\left. \begin{array}{c} \text{Corner} \\ \text{Force} \end{array} \right\} = \left[ \begin{array}{c} \text{Stiffness} \\ \text{Matrix} \end{array} \right] \left. \begin{array}{c} \text{Corner} \\ \text{Displacements} \end{array} \right\}$$

If, in the present problem of the bi-leaf cantilever, the common interface is divided into a number of points, each point will be split into two unmatched points by slip of the interface. It is assumed that the existence of clamping pressure will not allow separation but will permit slippage, of the two points. To find the damping energy is to find the work done by the slip friction action on the relative slip displacement of each pair of originally matched points.

The first model chosen in the finite element analysis was again a bileaf cantilever beam so that the result could be compared with Formula 13. For a direct comparison, numerical values were used. For either part of the beam, the length was taken as 10 inches, the depth 0.8 inches, and the width unity. The two-dimensional idealization of the finite elements of the model is shown in Figure 26. The clamping pressure on the bileaf beam was taken as 80 psi, the coefficient of friction of steel is presumably 0.14, and thus the interfacial shearing stress between the two parts is 11.2 lbs. per linear inch. The friction stresses were replaced by the resultant nodal shear forces. The 200 lbs. of free end load was evenly divided among the nodal points at the end.

Computer program tests for various kinds of idealizations of finite elements have shown that it is better to have finer elements at regions nearer to the fixed end. This is because the stresses are higher at those regions.

In the study made here, each part was divided into 456 elements and 273 nodal points. This made it necessary to solve 546 linear simultaneous equations. By avoiding the storage of the zero terms, the 546 x 546 stiffness matrix was reduced to only 546 x 35 terms, which is within the capacity of the CDC 1604 computer used.

The computer output gave the relative slip displacement of each pair of originally matched points on the interface. Having the nodal resultant shearing forces at the interface and their corresponding slip displacements, the slip damping energy of a quarter of a cycle was found to be 0.1889 in-lbs. For a complete cycle it is 0.7556 in-lbs. Comparing the computer result with the answer from Formula (13), 0.880 in-lbs per cycle, the difference is 13.8%. The result obtained from Formula (13) is considered to be the more accurate one. The difference is mainly the result of shortcomings in the finite element idealization. Further developments in the selection and proportioning of elements should make it possible to obtain more accurate results using this technique and permit extending it to more complex problems.

CONCLUSIONS. Following are the major conclusions to be drawn from this investigation:

1. Short of a major inventive breakthrough in the design or configuration of welded joints, there appears to be no chance of obtaining sufficient

energy dissipation in a welded joint to have a significant noise reducing effect.

2. Substantial amounts of energy can be dissipated in bolted joints. Nevertheless, the obtainment of very low values of  $Q$  in bolted structural joints appears very doubtful.
3. Theoretically, there is an optimum value of bolt clamping pressure which will produce the greatest energy dissipation for a given configuration. The tests reported herein indicate that this optimum clamping pressure is so low that it would only exist in joints which would be too loose for ordinary structural purposes. That is, they would be joints in which an excessive amount of slip could occur under working loads.
4. Regardless of its effect on noise radiation, damping in bolted joints is an important source of energy dissipation. It should be studied further because of its general influence on structural response to dynamic loads.
5. The brief study made of the application of finite element techniques to the energy dissipation problem indicates that this is a promising area of further research.

ACKNOWLEDGEMENTS. Major portions of this report are based on the work and writing of Doctor Robert O. Fehr, Doctor Samuel J. Errera, and Mr. Henry T. Y. Yang. Their contributions are gratefully acknowledged.

REFERENCES

1. Fehr, R. O., Determination of the Specific Damping Energy of Ship Hull Joints, and its Effect on Noise Radiation, Technical Report I, July 30, 1964, Cornell University, Ithaca, N. Y.
2. Yang, H., Errera, S. J., and McGuire, W., Determination of the Specific Damping Energy of Ship Hull Joints, and its Effect on Noise Radiation, Progress Report, October 31, 1966, Cornell University, Ithaca, N. Y.
3. Den Hartog, Mechanical Vibrations, 4th Edition, McGraw-Hill Co., 1962.
4. a) Rowett, F. E., Elastic Hysteresis in Steel, Proc. of the Royal Society of London, Series A, Vol. 89, 1914, p. 528.  
b) Lazan, B. J., Energy Dissipation Mechanisms in Structures, with Particular Reference to Material Damping, Structural Damping, ASME, 1959.
5. Goodman, L. E., A Review of Progress in Analysis of Interfacial Slip Damping, Structural Damping, ASME, 1959.
6. Pian, T. H., Hallowell, F. C., Structural Damping in a Simple Built-up Beam, 1st Overseas National Congress of Applied Mechanics, June 1951.
7. Crandall, S. H., Random Vibration, J. Wiley & Sons, 1958.

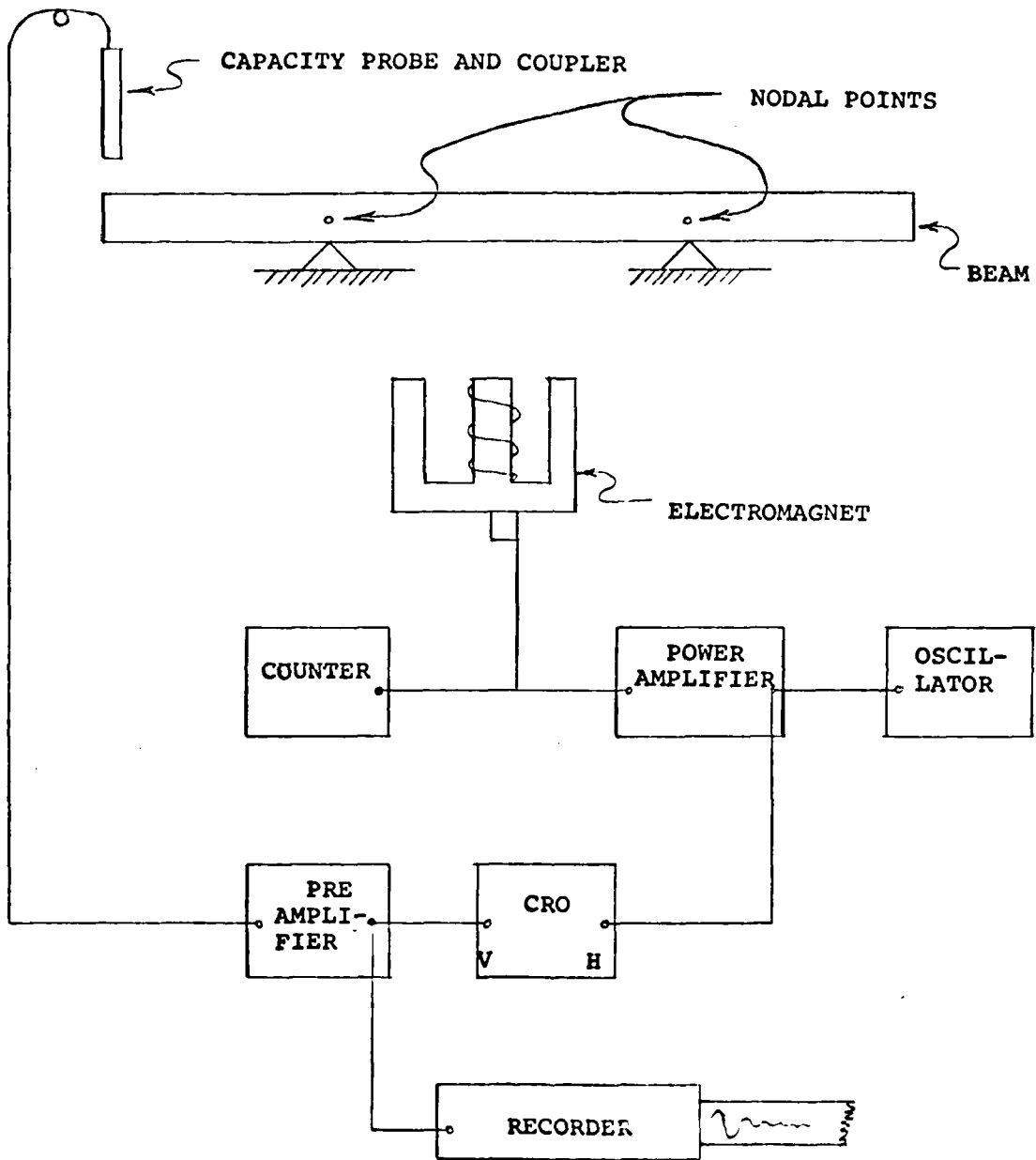


Figure 1

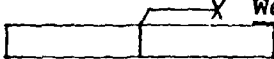
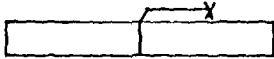
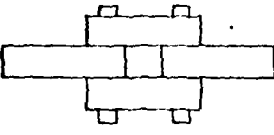
	Type	$\Omega$	$f_n$ (cps)
			
$4 \times \frac{5}{16} \times 25.5$	Integer	6200	99.8
<u>Welded Joints</u>			
	Butt welded Steel weld	4800	102
$4 \times \frac{5}{16} \times 25.5$			
	Butt welded Steel weld	1540	119.2
$3 \frac{1}{2} \times \frac{3}{8} \times 25.5$			
	Butt welded Lead filler	297	101.4
$3 \frac{1}{2} \times \frac{3}{8} \times 25.5$			
	Lap welded Steel weld	2050	121.6
$3 \frac{1}{2} \times \frac{3}{8} \times 25.5$			
<u>Bolted Joints</u>			
	Lap bolted	240-1000	113-115
$3 \frac{1}{2} \times \frac{3}{8} \times 25.5$ (3 bolts $\frac{3}{8}$ ")		(depending on bolt torque, amplitude, and surface roughness, see Figs. 3, 4, 5, 8, 9)	
	Bolted Butt Joint	50-500	113.3
$3 \times \frac{3}{8} \times 25.5$ (6 bolts $\frac{3}{8}$ ")		(depending on bolt torque)	

Figure 2  
Continued on next page.

Figure 2 - Continued

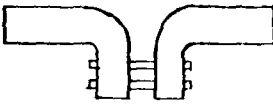
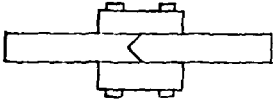
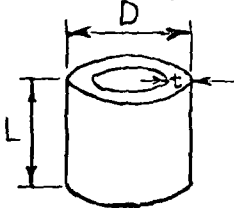
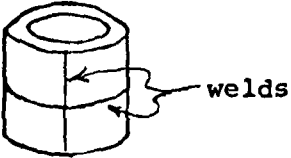
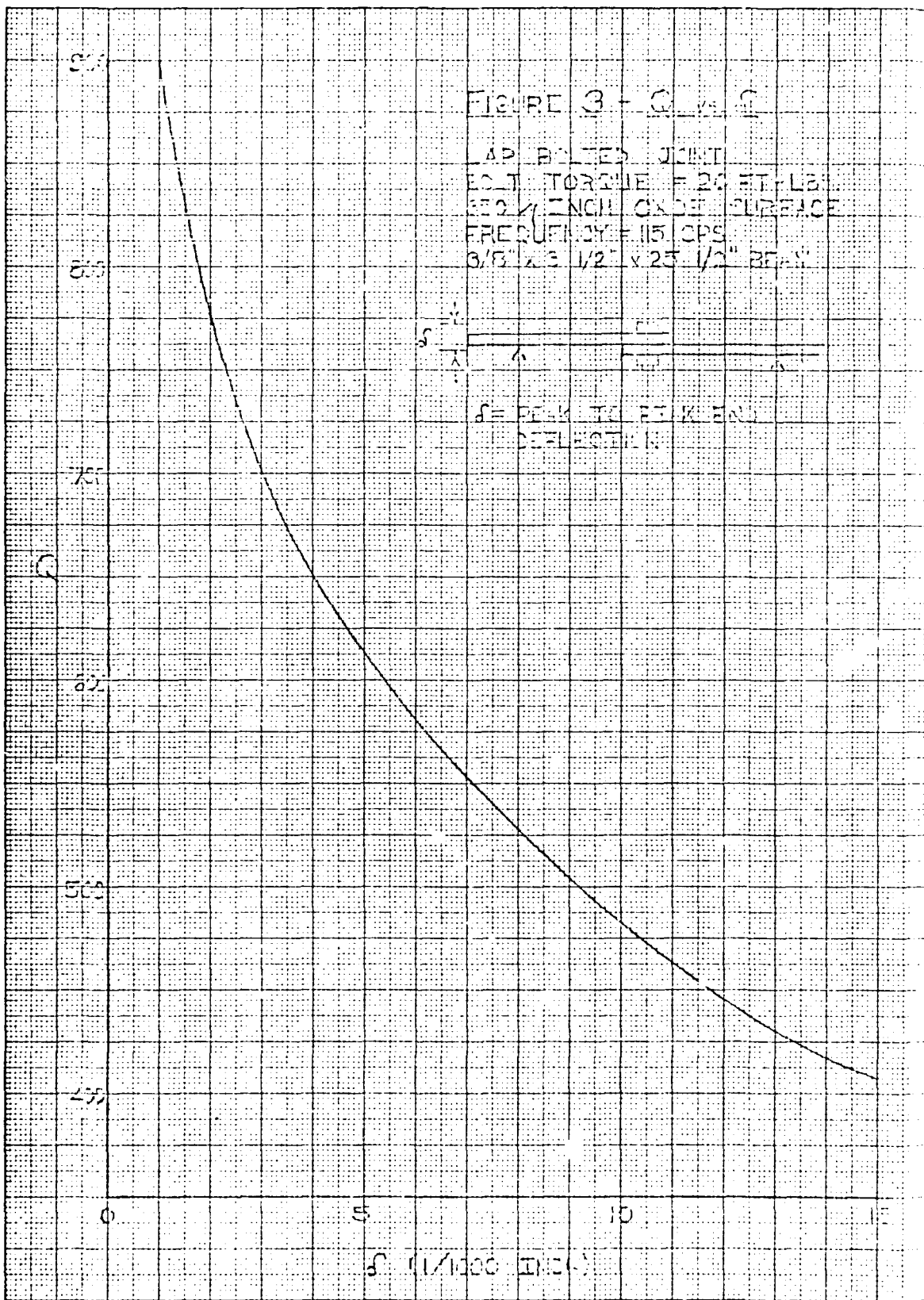
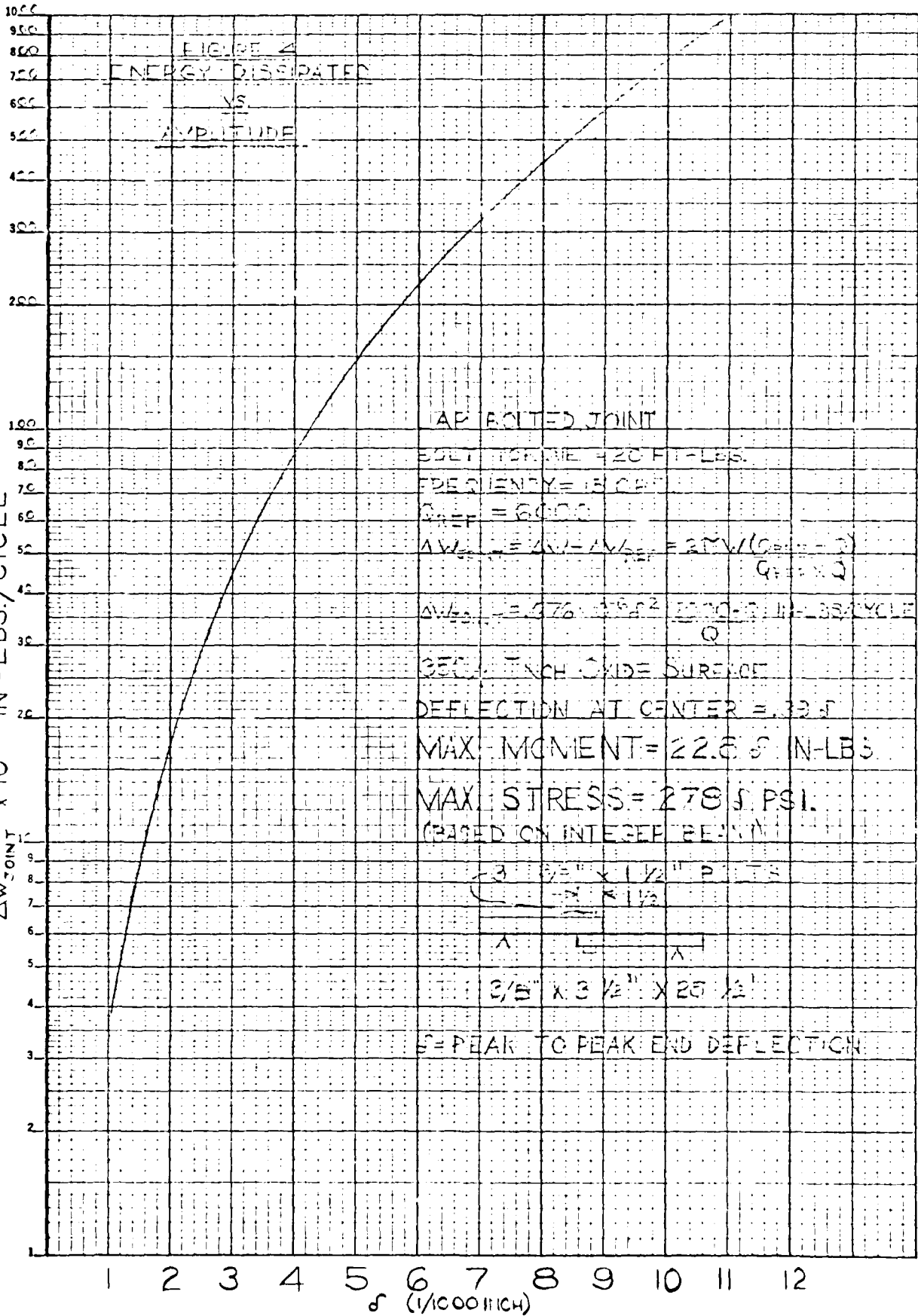
<u>Type</u>	<u>Q</u>	<u>f<sub>n</sub></u> (cps)
 Bolted Joint $3\ 1/2" \times \frac{3}{8}" \times 25.5"$ (6 bolts $\frac{3}{8}"$ )	470	152
 V-Bolted Butt Joint $3\ 1/2" \times \frac{3}{8}" \times 25.5"$ (6 bolts $\frac{3}{8}"$ )	500-1300	116 (depending on bolt torque [see Figs. 6, 7], amplitude and compressive force F.)
 <u>Cylinder</u> Integer $D = 8.36"$ $t = .28"$ $L = 7.5"$	2220	401
 $D = 10.5"$ $t = .35"$ $L = 7"$	1580	345

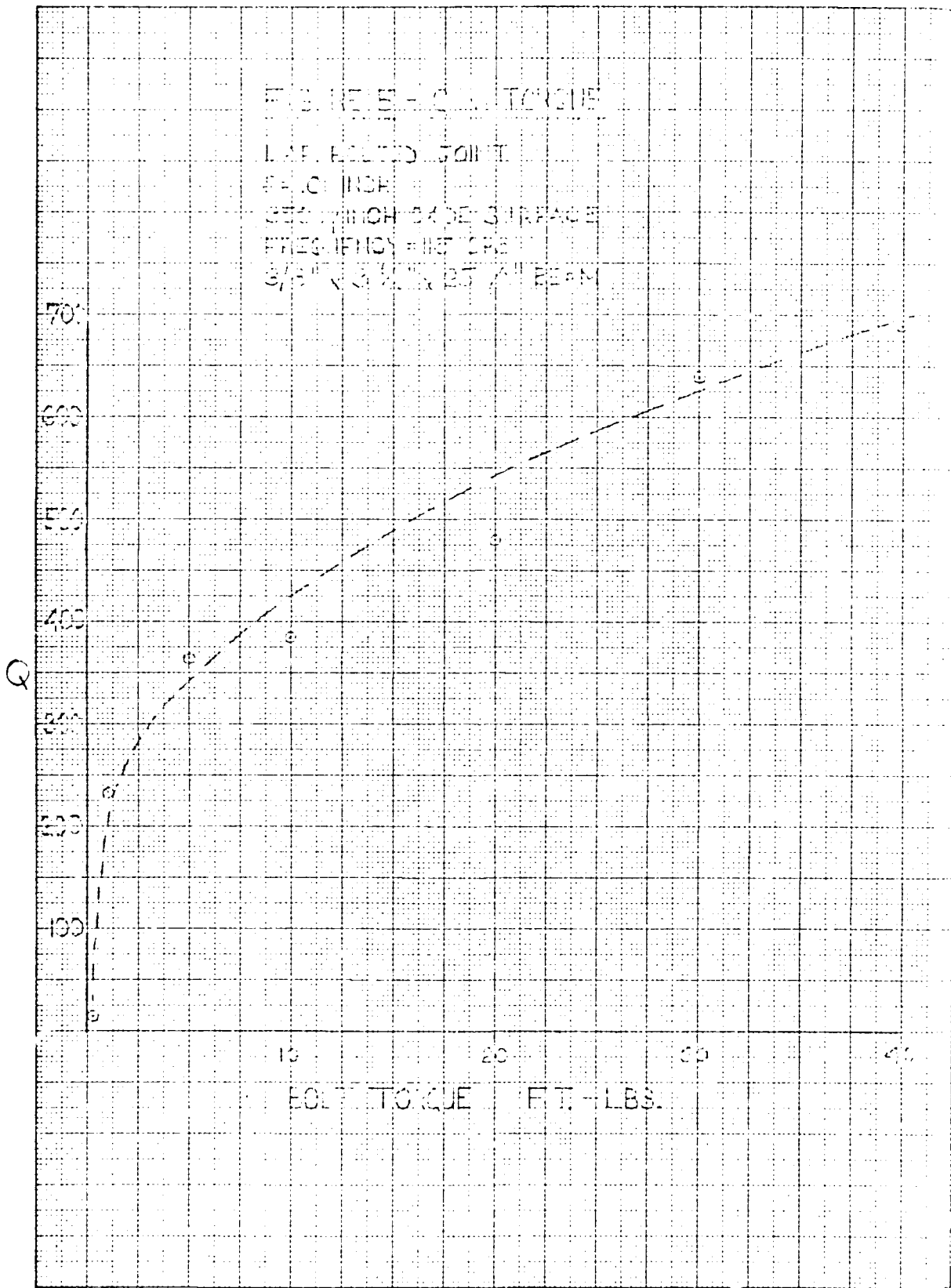
Figure 2

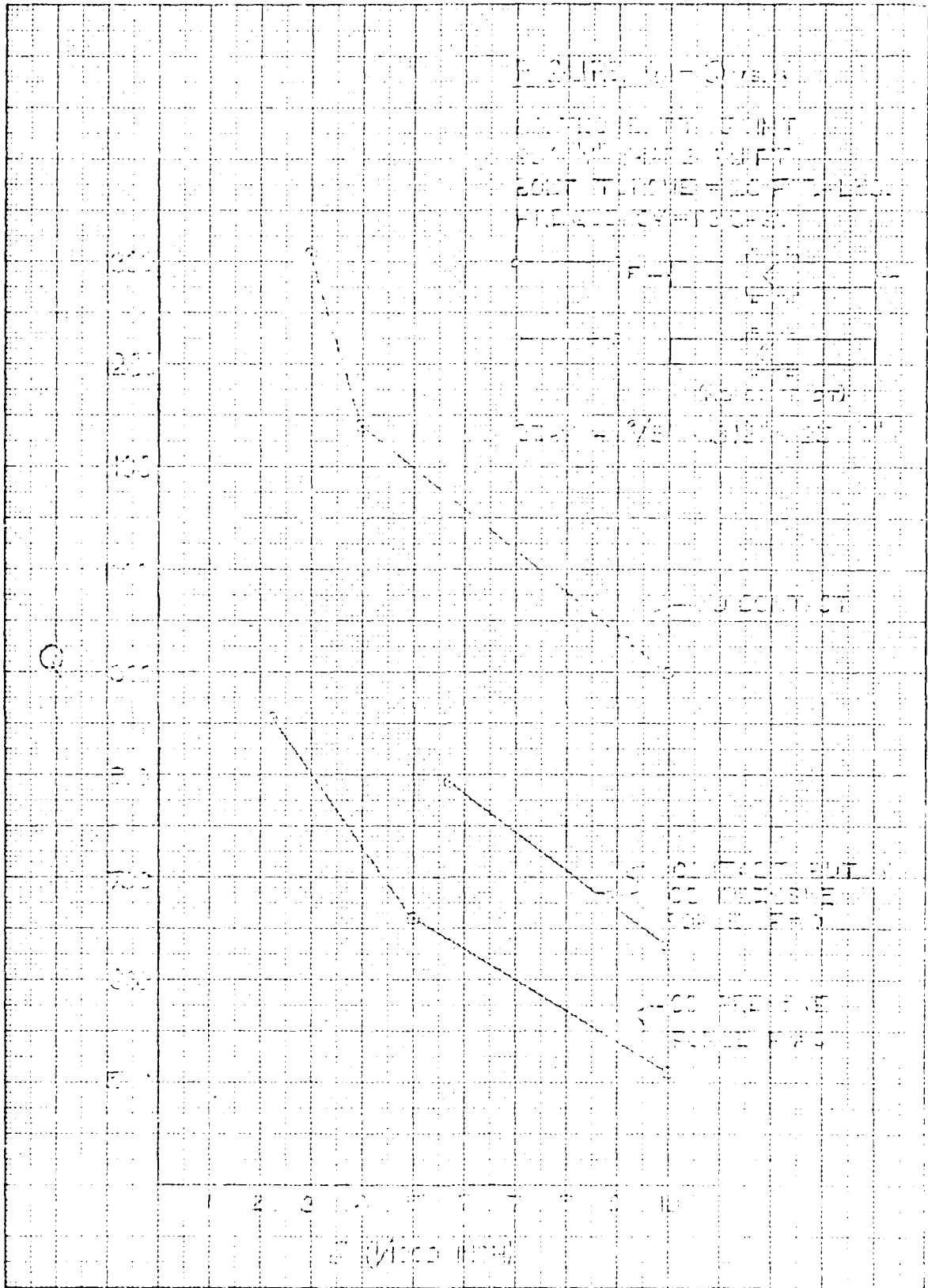


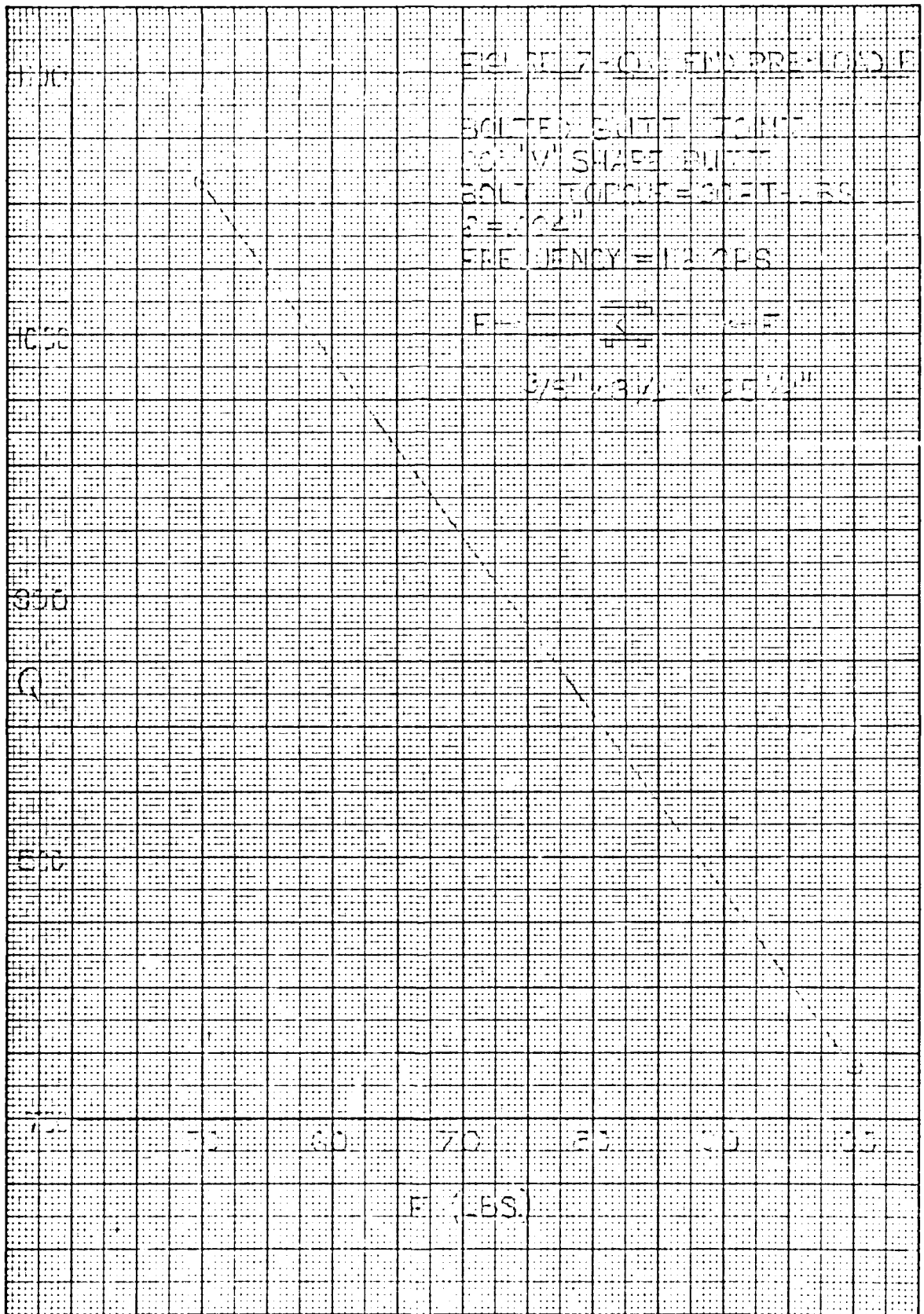
K&S SEMI-LOGARITHMIC 46 5493  
 3 CYCLES X 70 DIVISIONS. MADE IN U.S.A.  
 KEUFFEL & ESSNER CO.

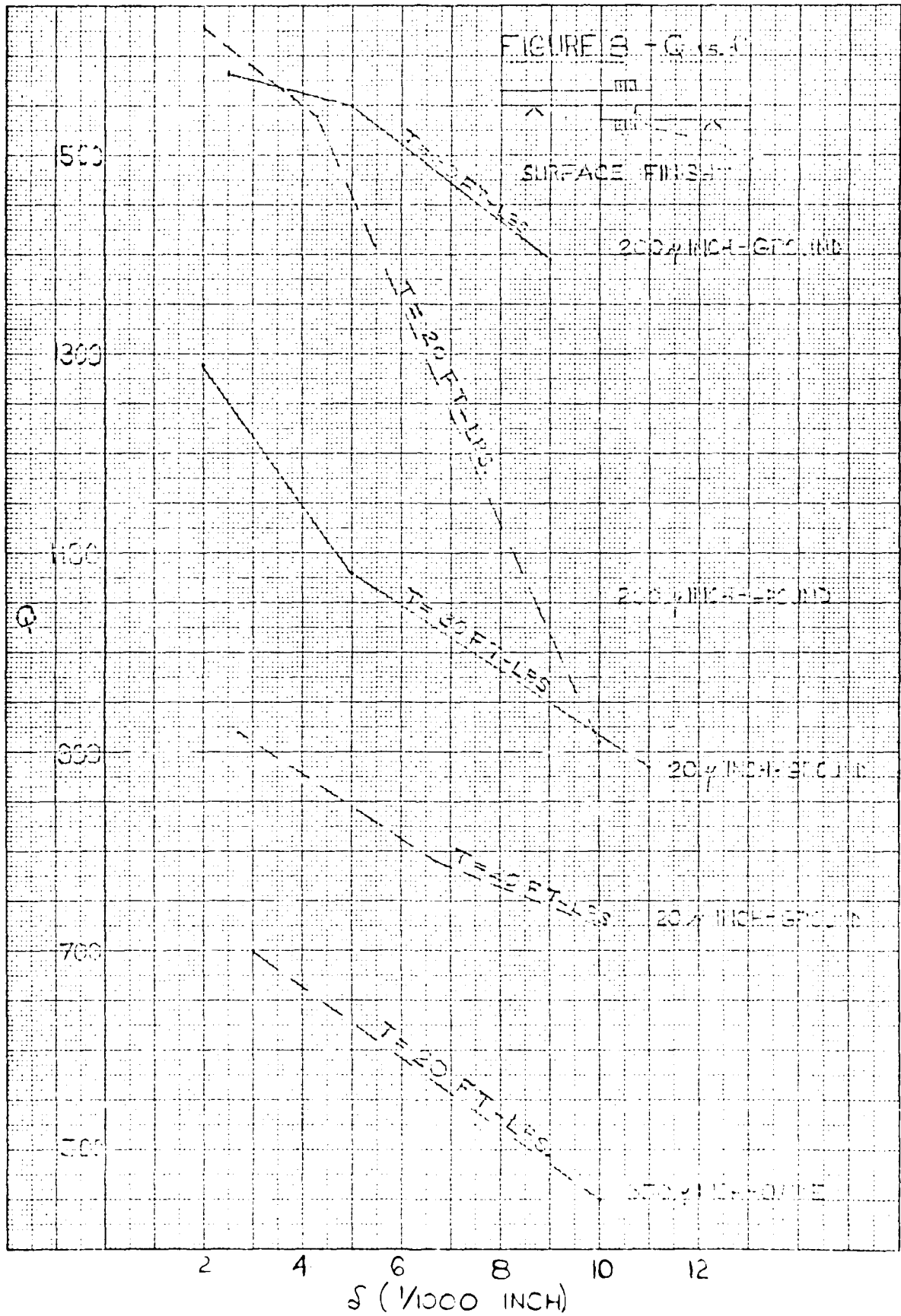
$\Delta W_{JOINT} \times 10^{-6}$  IN-LBS./CYCLE





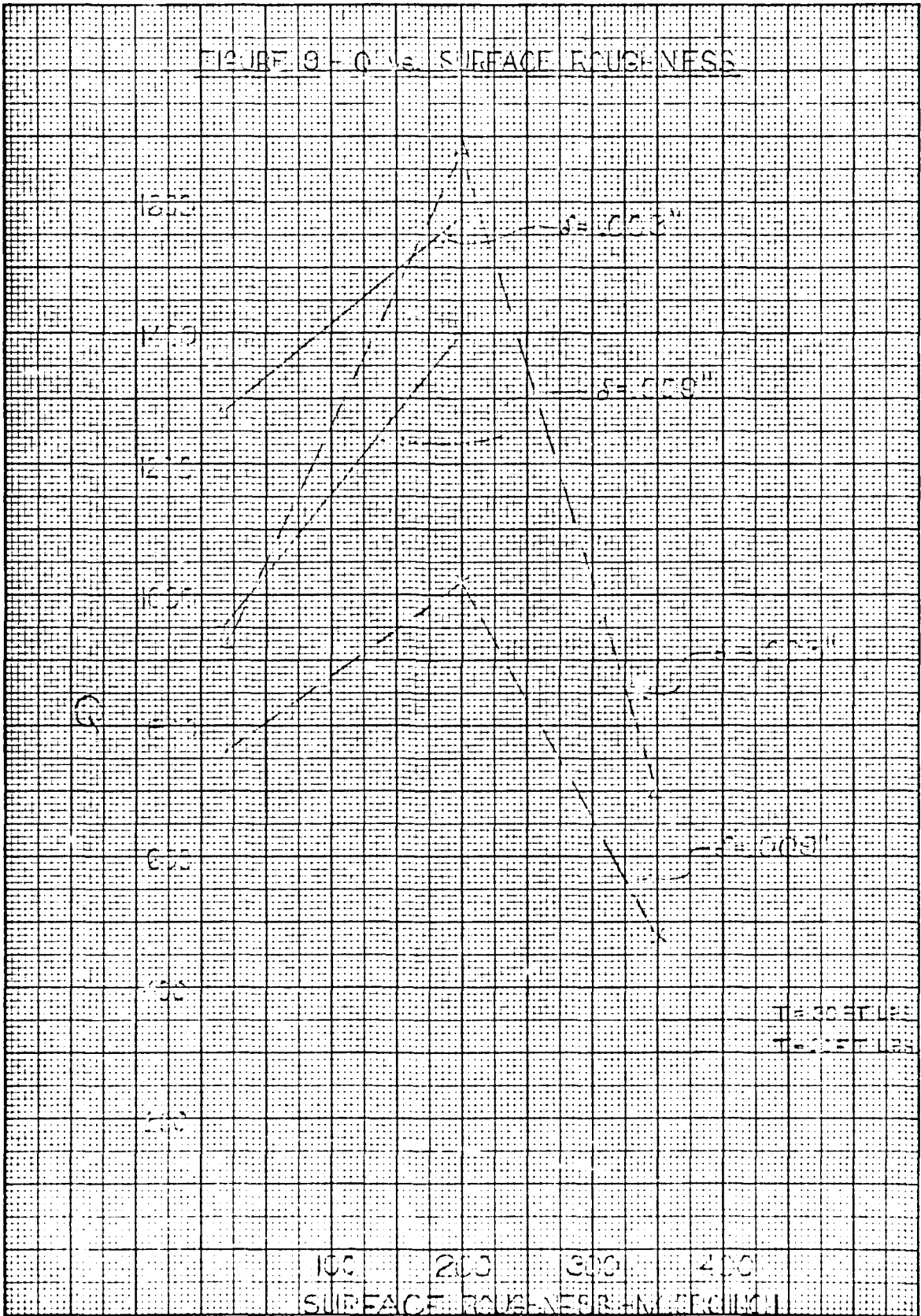






K-E 10 X 10 TO 1/2 INCH 46 1323  
 7 X 10 INCHES MADE IN U.S.A.  
 KEUPPEL & EBER CO.

FIGURE 9 - Q vs. SURFACE ROUGHNESS



TARGET LPS  
 TARGET LPS

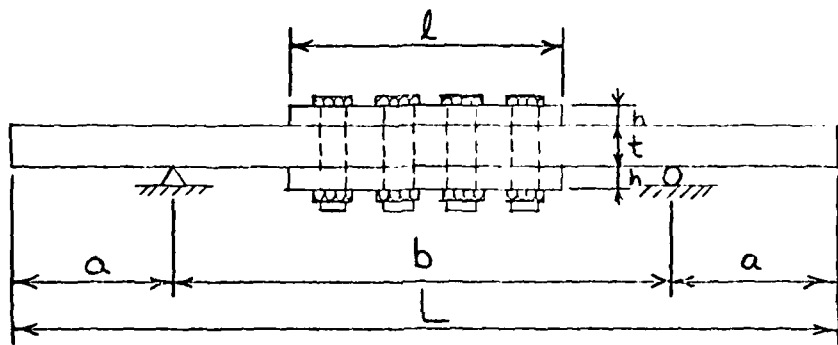


FIGURE 10

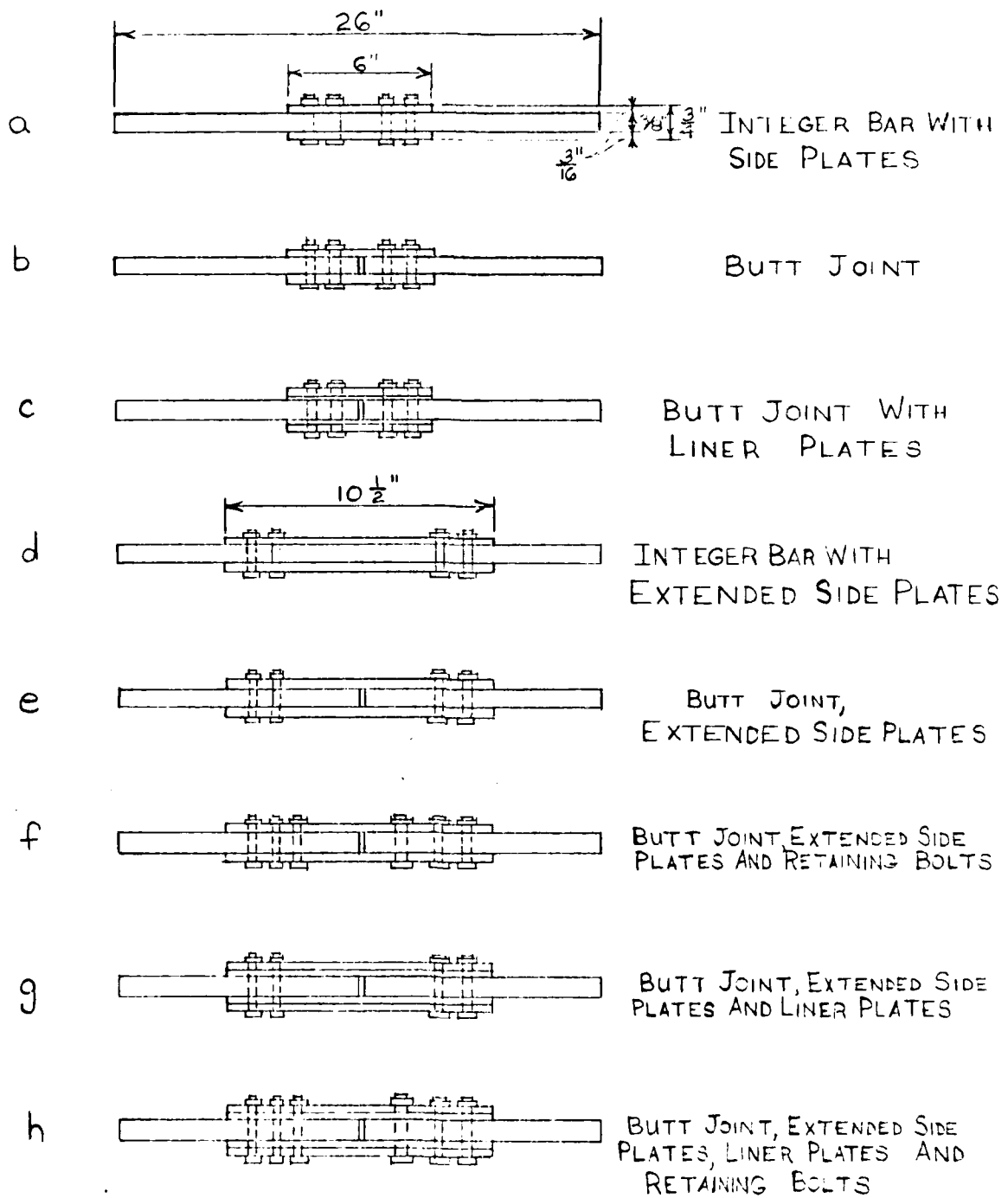
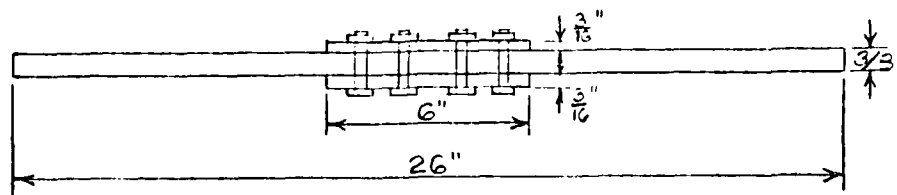
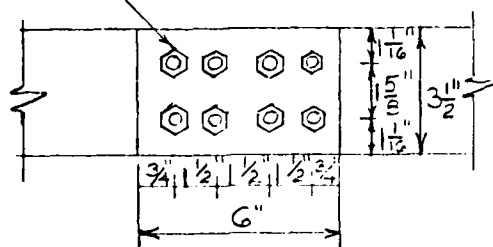


FIGURE II - TEST SPECIMENS

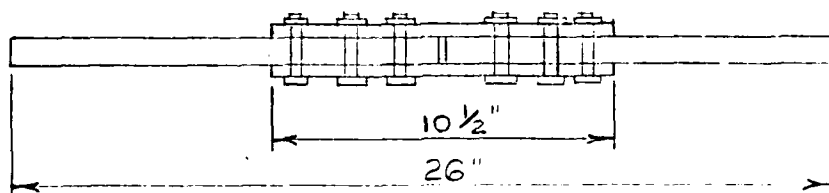
SPECIMEN "a"



8 - 1/2" H.S. BOLTS  
9/16" HOLES



SPECIMEN "f"



10 - 1/2" H.S. BOLTS  
9/16" HOLES

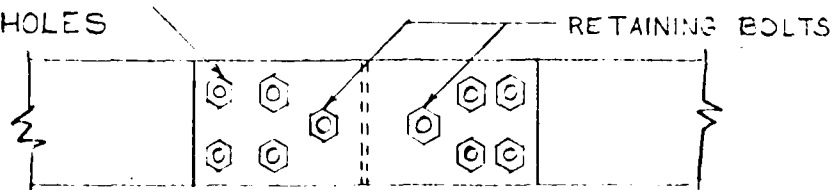


FIGURE 12 - DETAIL OF TWO TYPICAL SPECIMENS

K&E 10 X 10 TO 1/2 INCH 46 1323  
 7 X 10 INCHES MADE IN U.S.A.  
 KEUFFEL & ESSER CO.

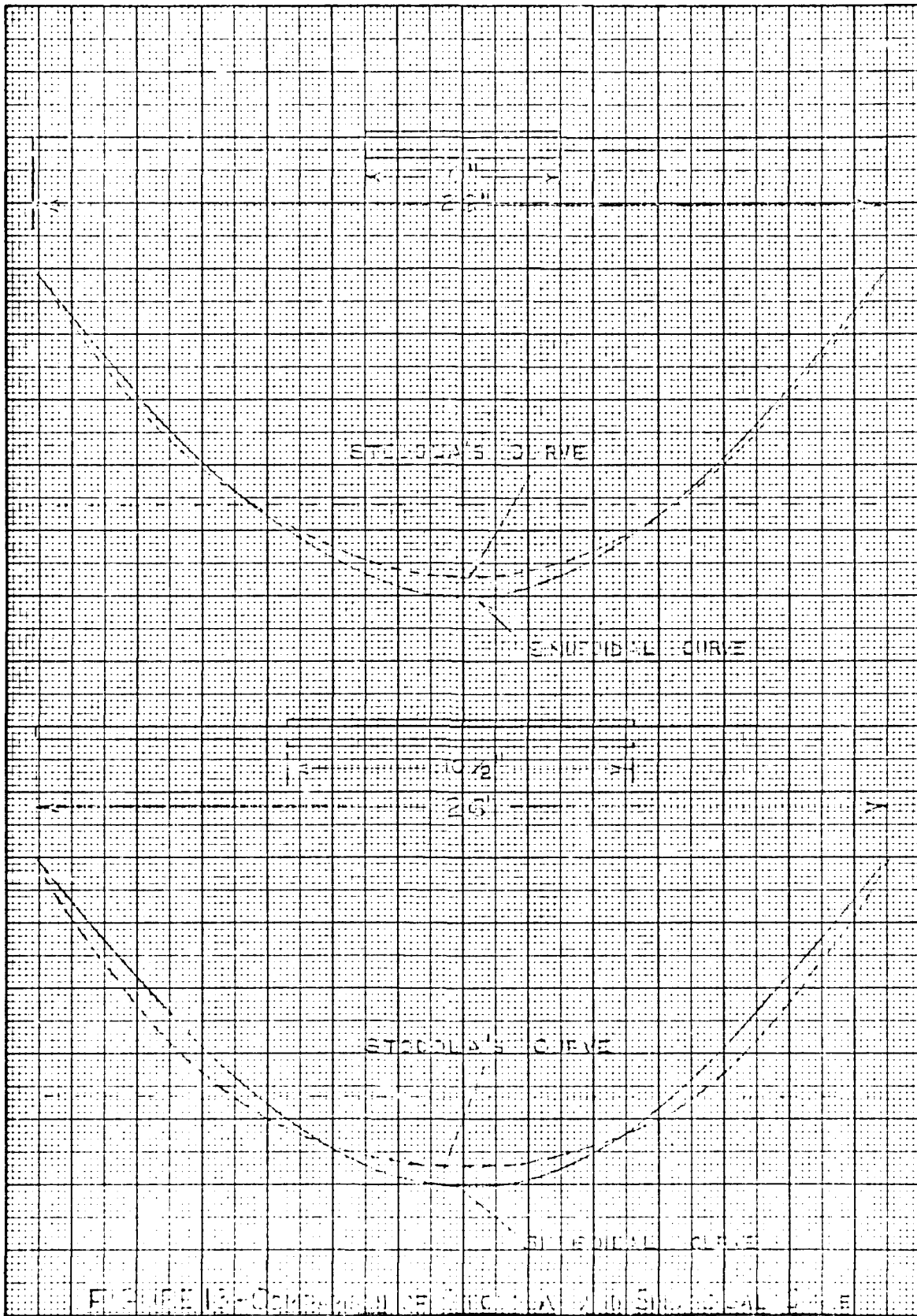


FIGURE 13—COMPARISON OF STODOLA'S CURVE AND EQUIDISTANT CURVE

LOGARITHMIC 46 7403  
3 X 5 CYCLES  
KEUFFEL & ESSER CO.

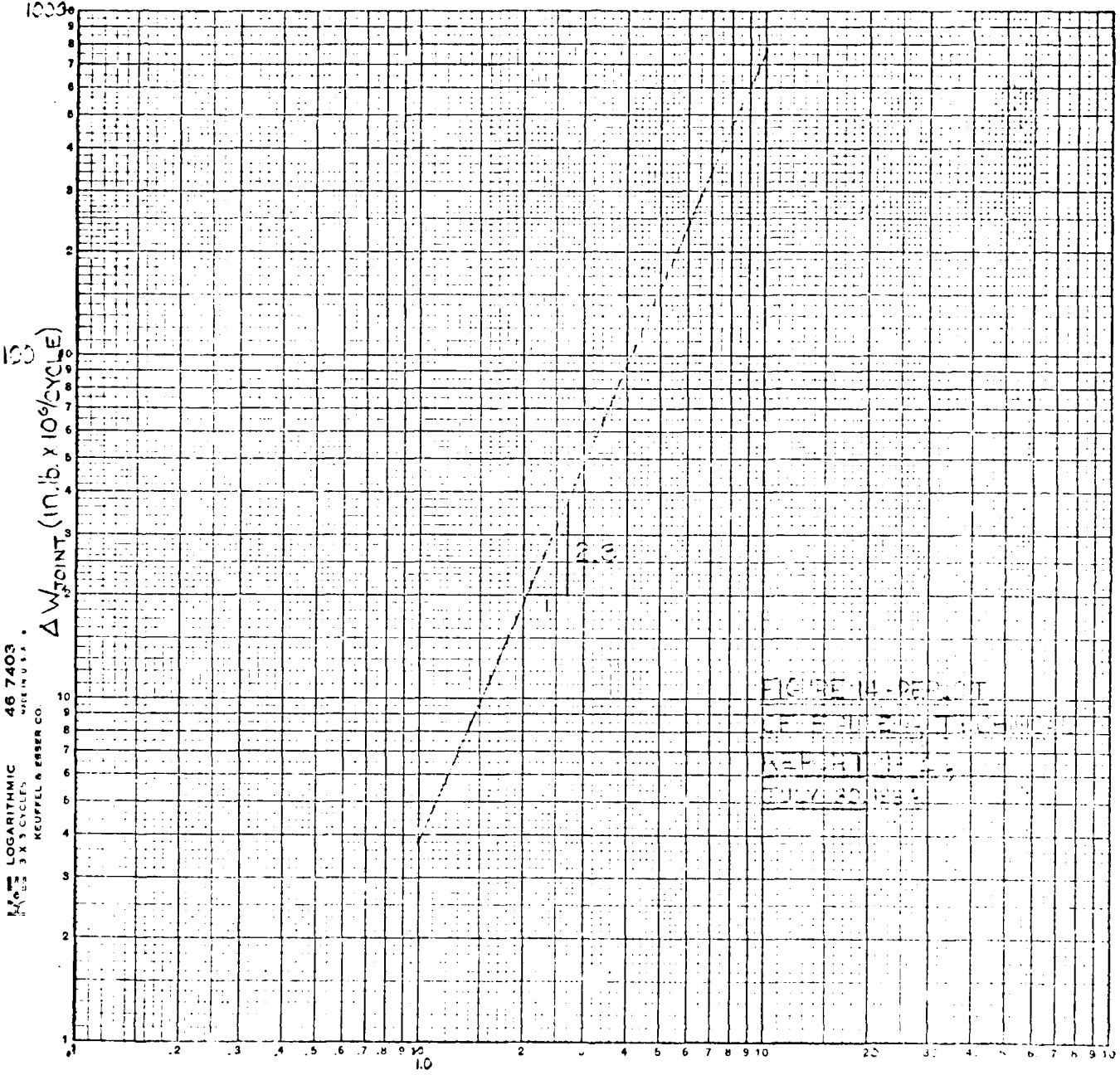
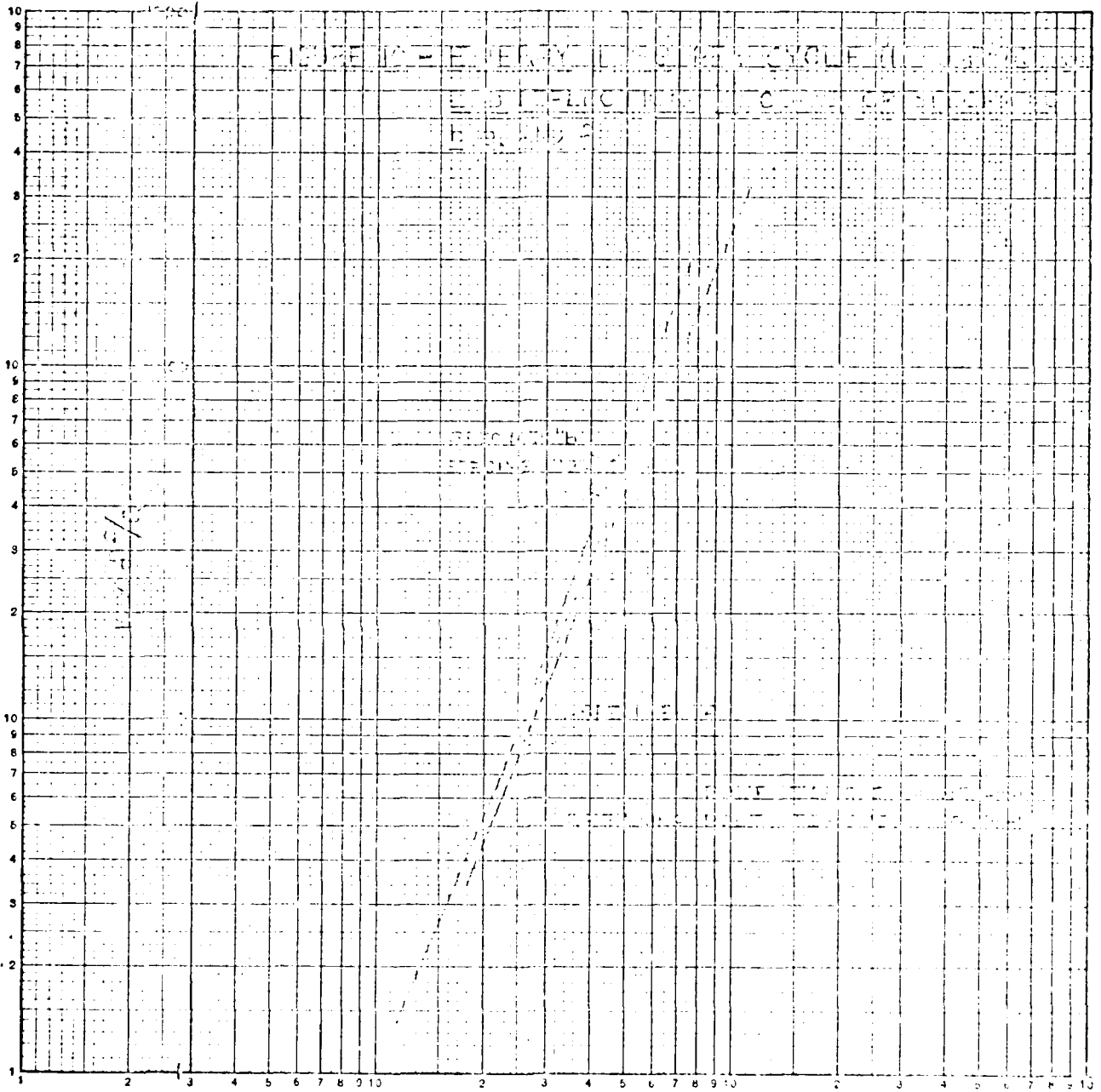


FIGURE 14 - PERIOD  
RESEARCH INSTITUTE  
REPORT 11-1-3  
JULY 30 1939

$\delta$  (IN.  $\times 10^3$ )  
GRAPHIC NOT REPRODUCIBLE

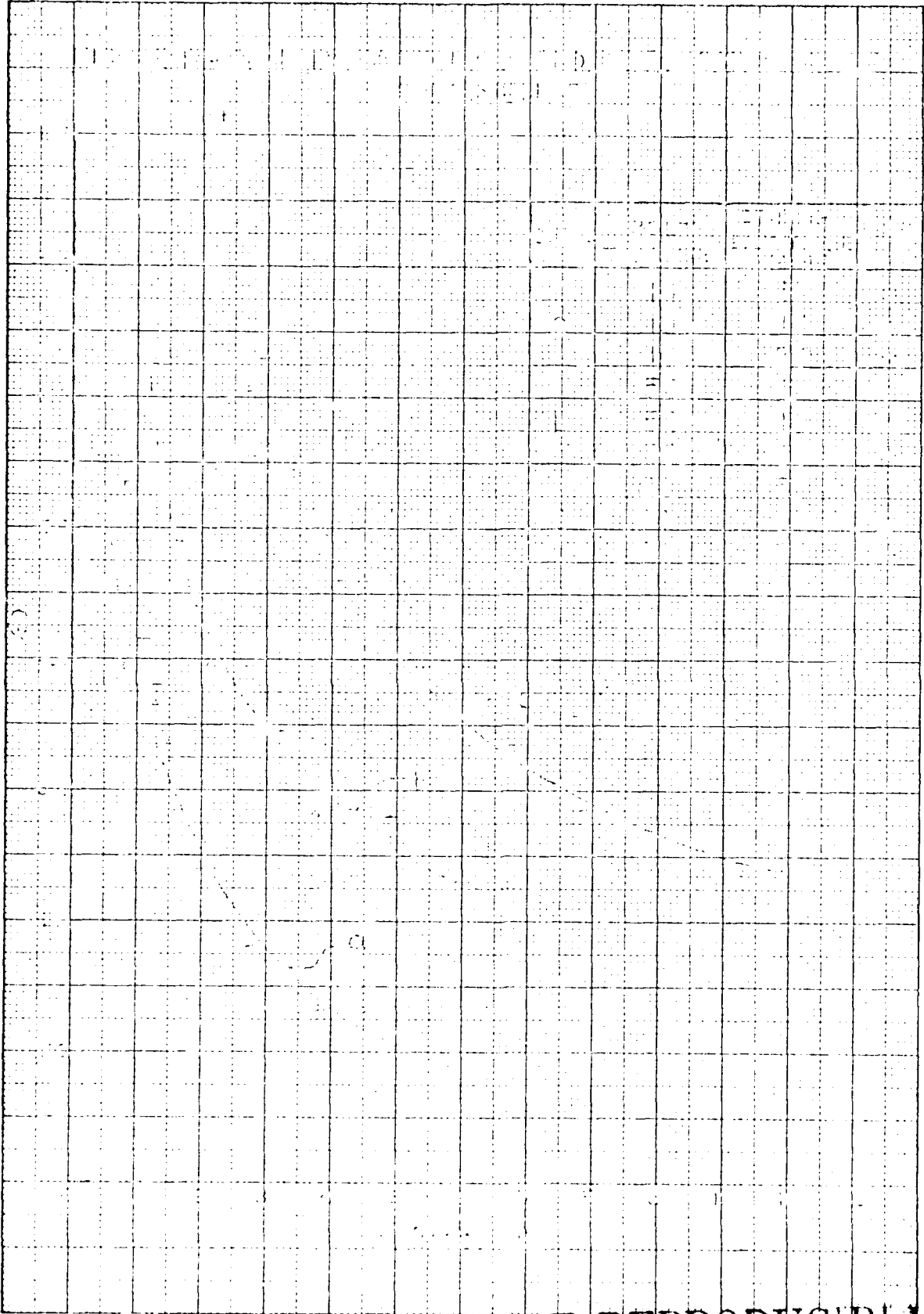


# GRAPHIC NOT REPRODUCIBLE

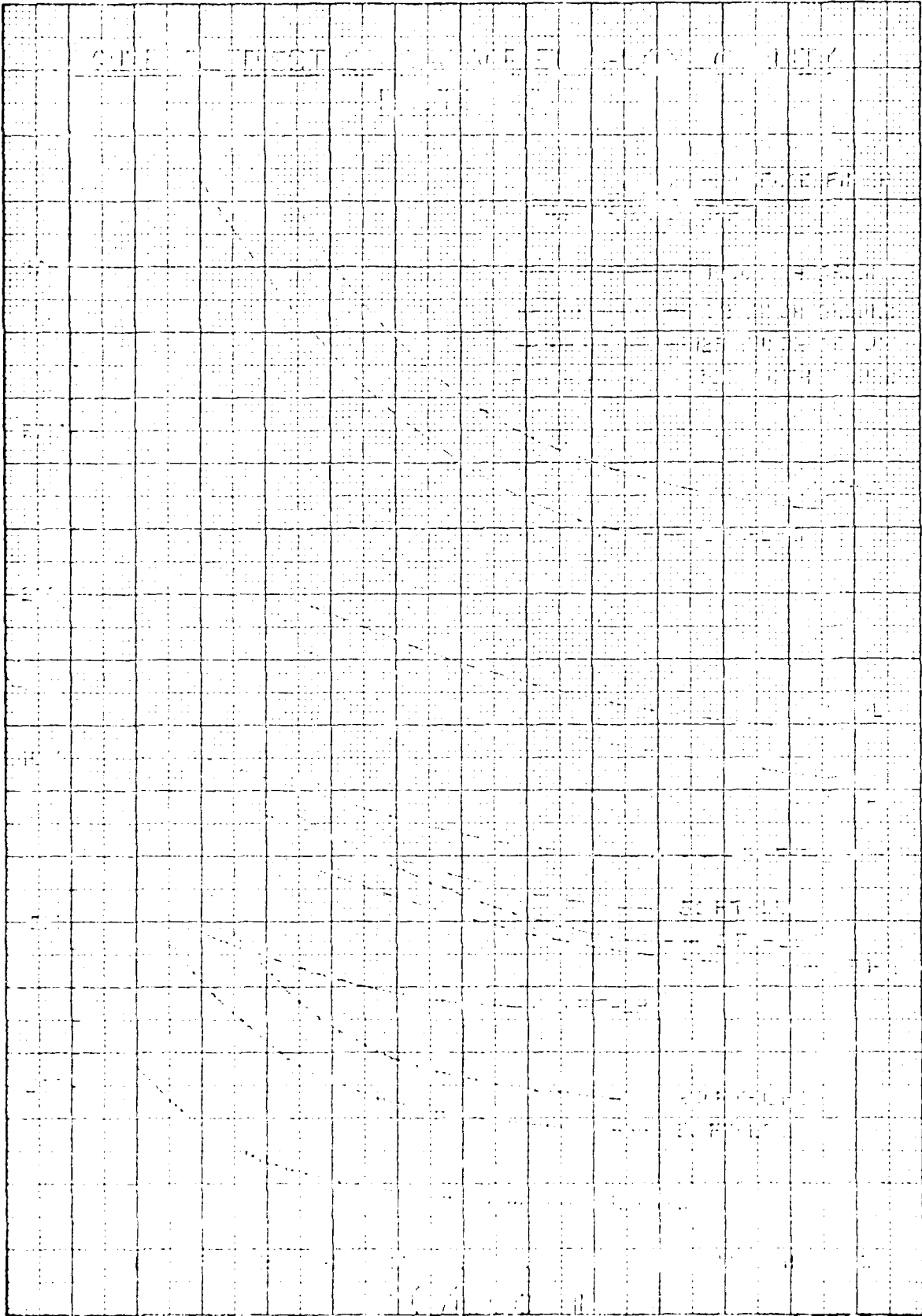


LOGARITHMIC 46 7403  
KEUFFEL & ESSER CO.

$\delta$  (1/100 IN)



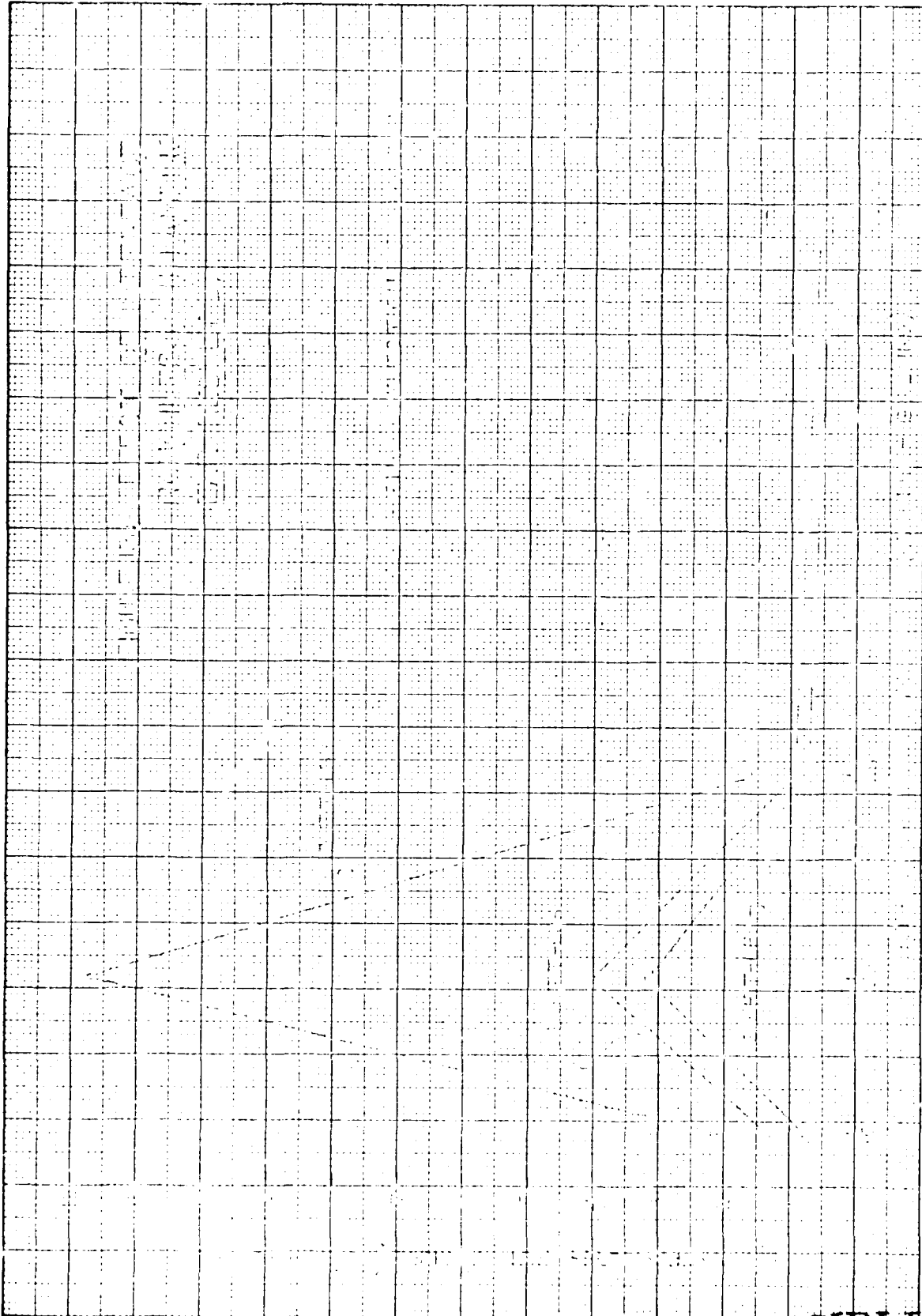
GRAPHIC NOT REPRODUCIBLE



KEUFFEL & ESSER CO.

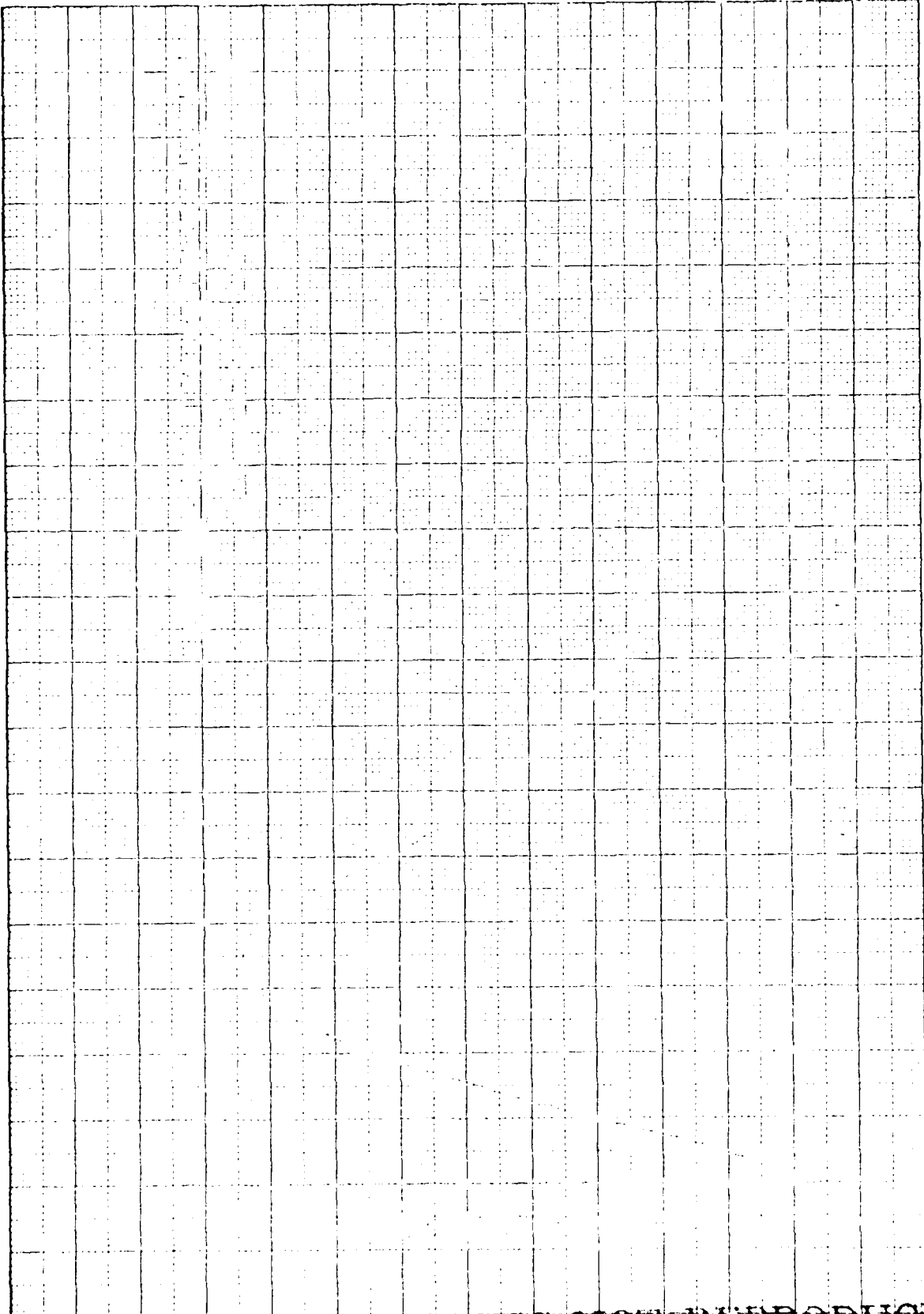
GRAPHIC NOT REPRODUCIBLE

1/2" 10 X 10 TO 1/2" INCH 46 1323  
7 3/10 INCH  
KEUFFEL & ESSER CO.  
NEW YORK, N. Y.



GRAPHIC NOT REPRODUCIBLE

10 X 10 TO 1/2 INCH 46 1323  
KUPFER & ESSER CO



GRAPHIC NOT REPRODUCIBLE

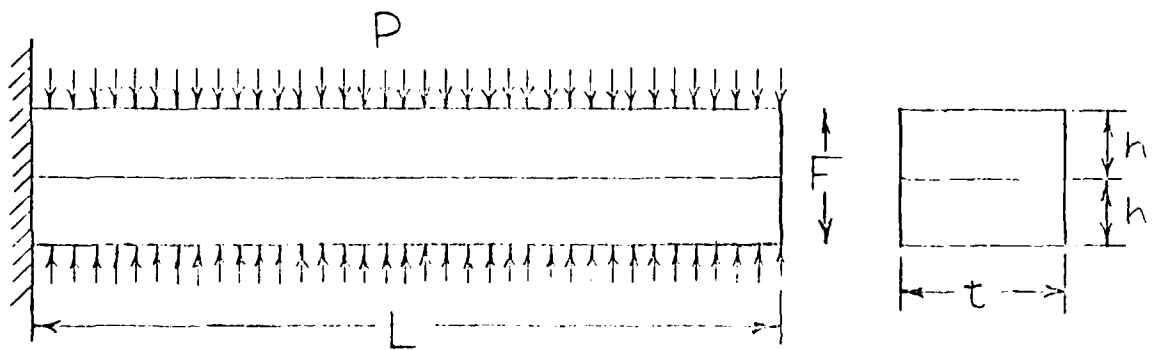


FIGURE 20 - BILINEAR CANTILEVER MODEL

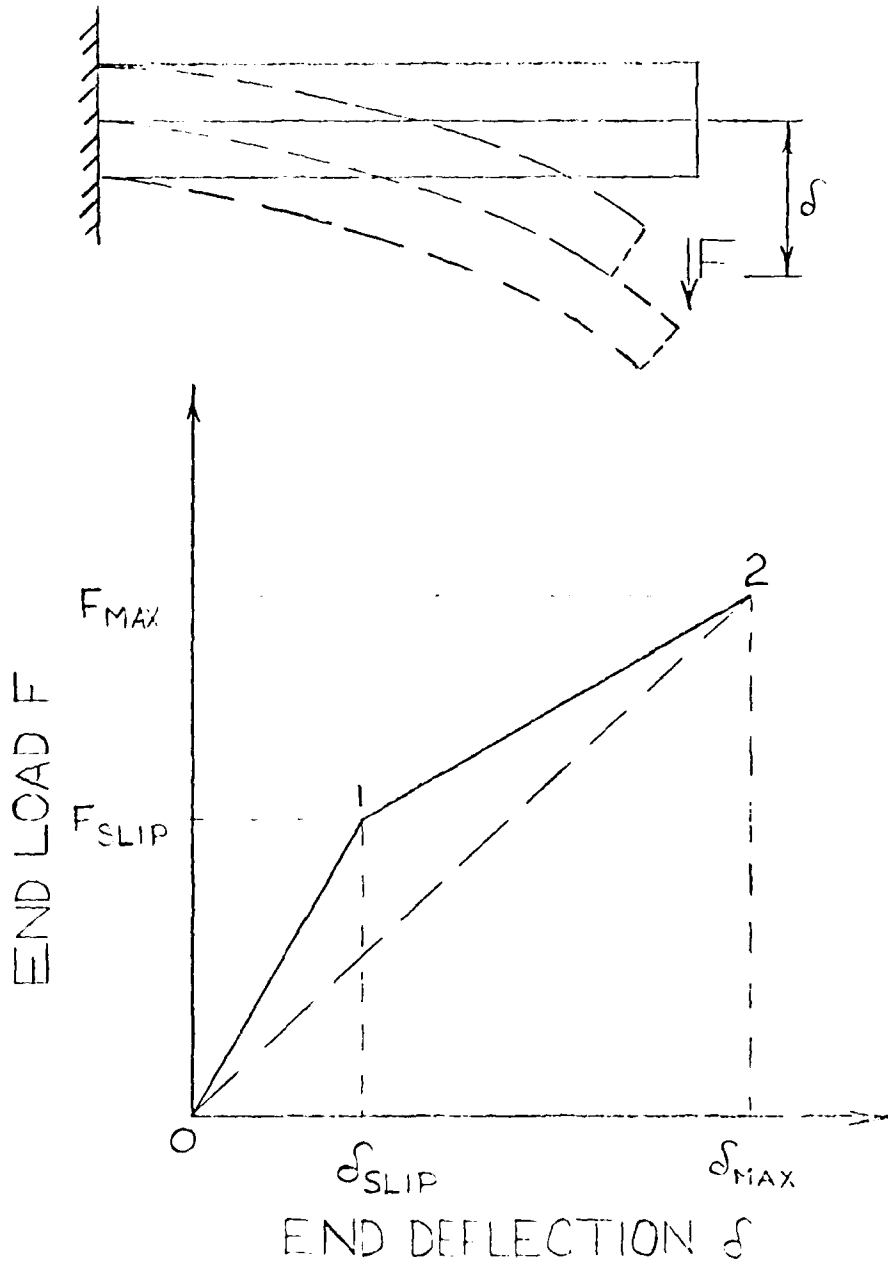


FIGURE 21-LOAD DEFLECTION RELATION

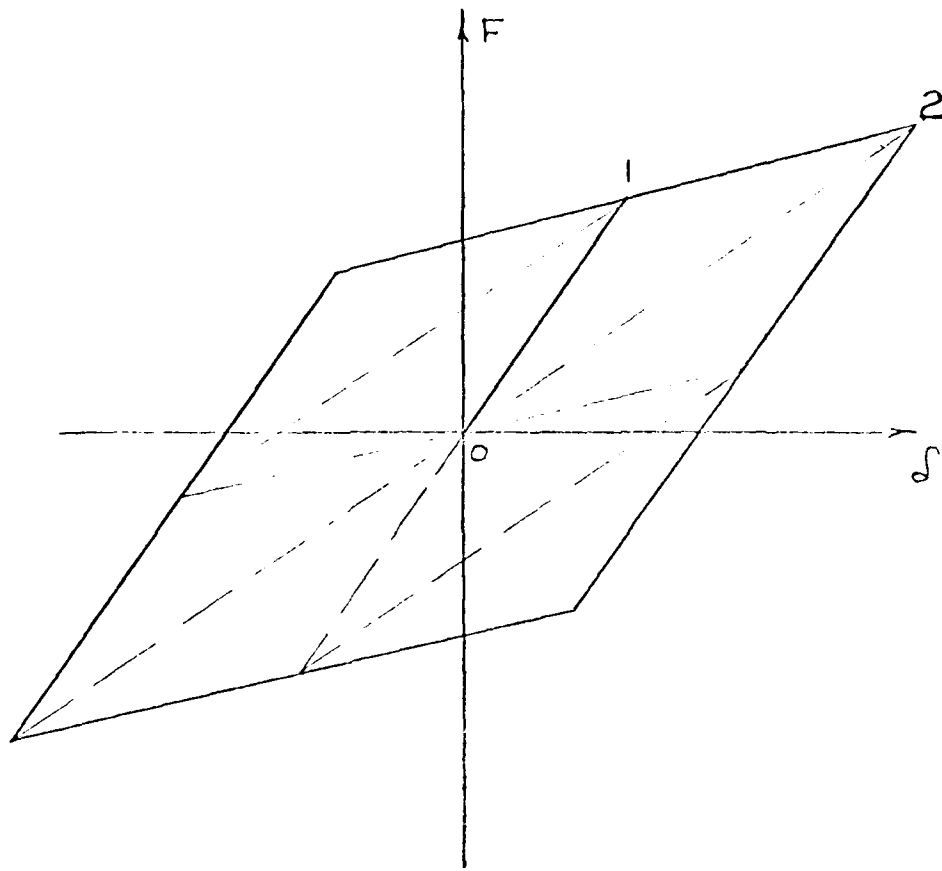


FIGURE 22 - A COMPLETE CYCLE  
OF LOAD-DEFLECTION RELATION

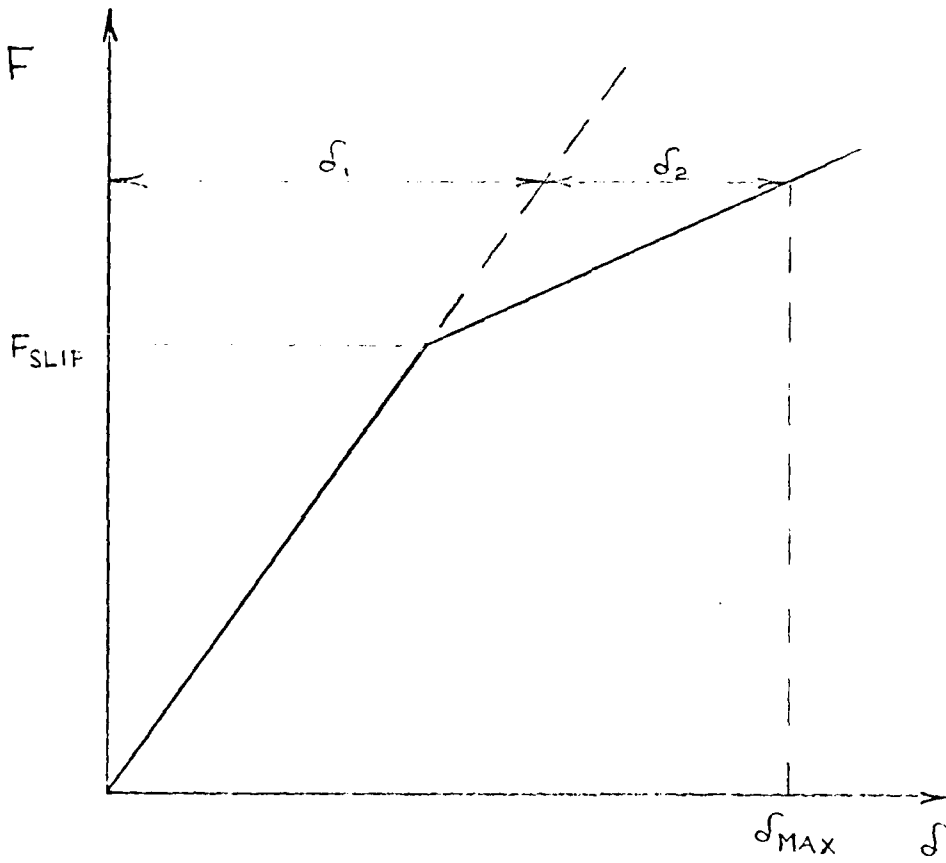


FIGURE 23 - SUPERPOSITION OF  $\sigma_1$  &  $\sigma_2$

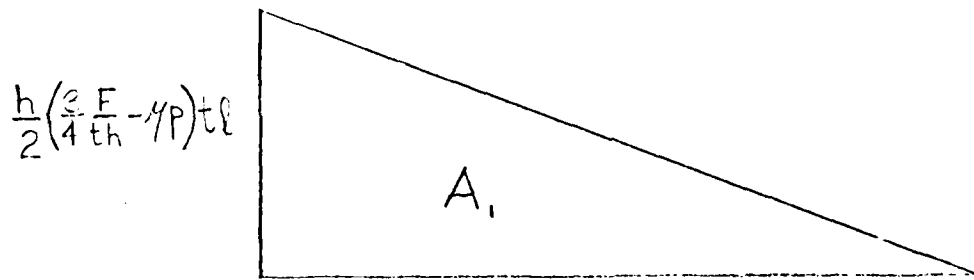
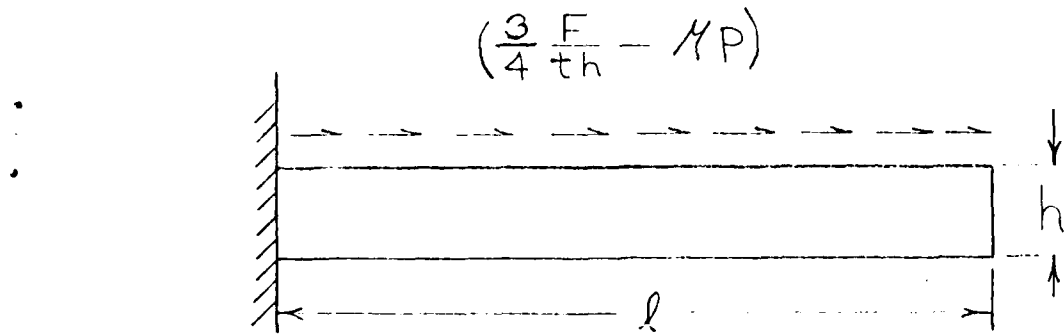


FIGURE 24 - LOADING & MOMENT DIAGRAM

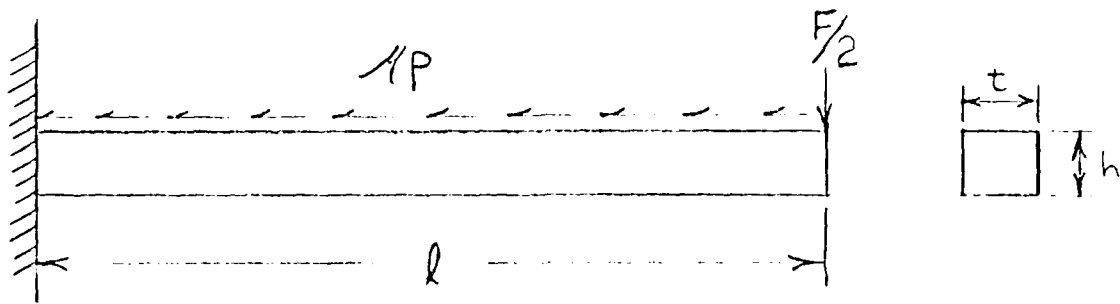
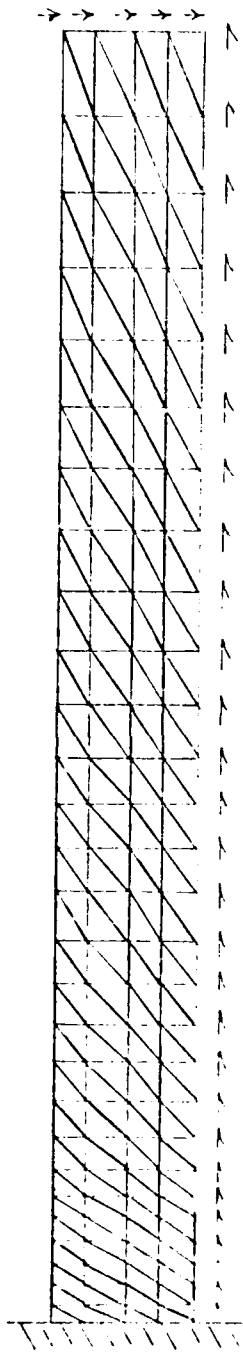
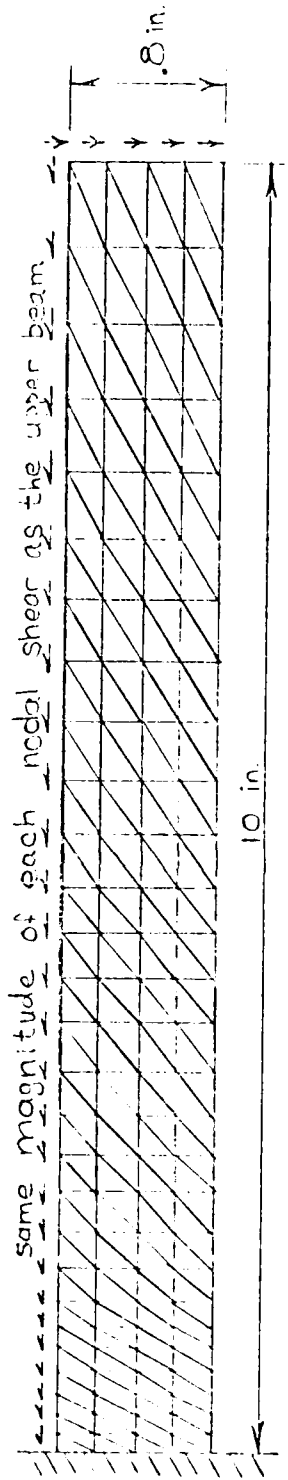


FIGURE 25-LOADING CONDITION FOR THE LOWER PART OF BILEAF BEAM



(UPPER LEAF)



(LOWER LEAF)

FIGURE 26 - IDEALIZATION OF THE BILEAF CANTILEVER BEAM